

YGS Open File 2023-1

# Surficial geology and geohazards of the greater Whitehorse area

P.S. Lipovsky



Published under the authority of the Department of Energy, Mines and Resources, Government of Yukon [yukon.ca](http://yukon.ca).

Printed in Whitehorse, Yukon, 2023.

Publié avec l'autorisation du Ministère de l'Énergie, des Mines et des Ressources du gouvernement du Yukon, [yukon.ca](http://yukon.ca).

Imprimé à Whitehorse (Yukon) en 2023.

© Department of Energy, Mines and Resources, Government of Yukon

This, and other Yukon Geological Survey publications, may be obtained from:

Yukon Geological Survey

102-300 Main Street

Box 2703 (K-102)

Whitehorse, Yukon, Canada Y1A 2C6

email [geology@gov.yk.ca](mailto:geology@gov.yk.ca)

Yukon Geological Survey website <https://yukon.ca/en/science-and-natural-resources/geology>.

In referring to this publication, please use the following citation:

Lipovsky, 2023. Surficial geology and geohazards of the greater Whitehorse area. Yukon Geological Survey, Open File 2023-1, 67 p. plus appendices.

Cover photo: Mudflow source zone on the upper slopes of the Whitehorse escarpment above Main Street. June 2020 photo by Panya Lipovsky. Photo by Panya Lipovsky.

Back photo: Takhini River retrogressive thaw flow, with the Alaska Highway in the background. September 2022 photo by Peter von Gaza.



**YGS Open File 2023-1**

**Surficial geology  
and geohazards of  
the greater  
Whitehorse area**

P.S. Lipovsky  
Yukon Geological Survey

# Table of Contents

<b>Introduction</b> .....	1
<b>Background setting</b> .....	2
Bedrock geology .....	2
Quaternary geology and landscape evolution .....	5
<b>Data sources and methods</b> .....	7
Field investigations .....	7
Lidar .....	7
Aerial photographs .....	8
Borehole data .....	8
Surficial geology and soil survey maps .....	9
Surficial geology mapping classification system .....	9
Surficial materials .....	9
Anthropogenic (A) .....	9
Organic (O) .....	12
Eolian (E) .....	12
Colluvium (C) .....	12
Fluvial (F) .....	15
Lacustrine (L) .....	16
Glaciolacustrine (LG) .....	17
Glaciofluvial (FG) .....	18
Morainal (M) .....	20
Bedrock (R) .....	21
Texture .....	22
Surface expression .....	23
Age .....	24
Geomorphological processes .....	24
<b>Spatial data</b> .....	25
Points .....	25
Lines .....	26
Polygons .....	27

<b>Geohazards</b> .....	28
Landslides .....	28
2022 Whitehorse escarpment slides .....	32
Historical background .....	34
Geological background .....	34
Landslide mechanisms .....	35
April 30, 2022 Robert Service Way slide .....	36
May 25, 2022 Drury Street slide .....	38
May 27, 2022 Wood Street slide .....	40
May 28, 2022 Jeckell Street slide .....	40
May 31, 2022 Robert Service Way slide #2 .....	43
Implications .....	43
Future research opportunities .....	44
Radon .....	45
Seismicity .....	47
Permafrost .....	49
Flooding .....	51
Aggregate potential analysis .....	54
Limitations .....	55
<b>Acknowledgements</b> .....	58
<b>References</b> .....	59
<b>Appendix 1 – Map sheets</b> .....	66
1:15 000 scale surficial geology maps .....	66
1:25 000 scale aggregate potential map .....	66
<b>Appendix 2 – Digital spatial data compilation</b> .....	67

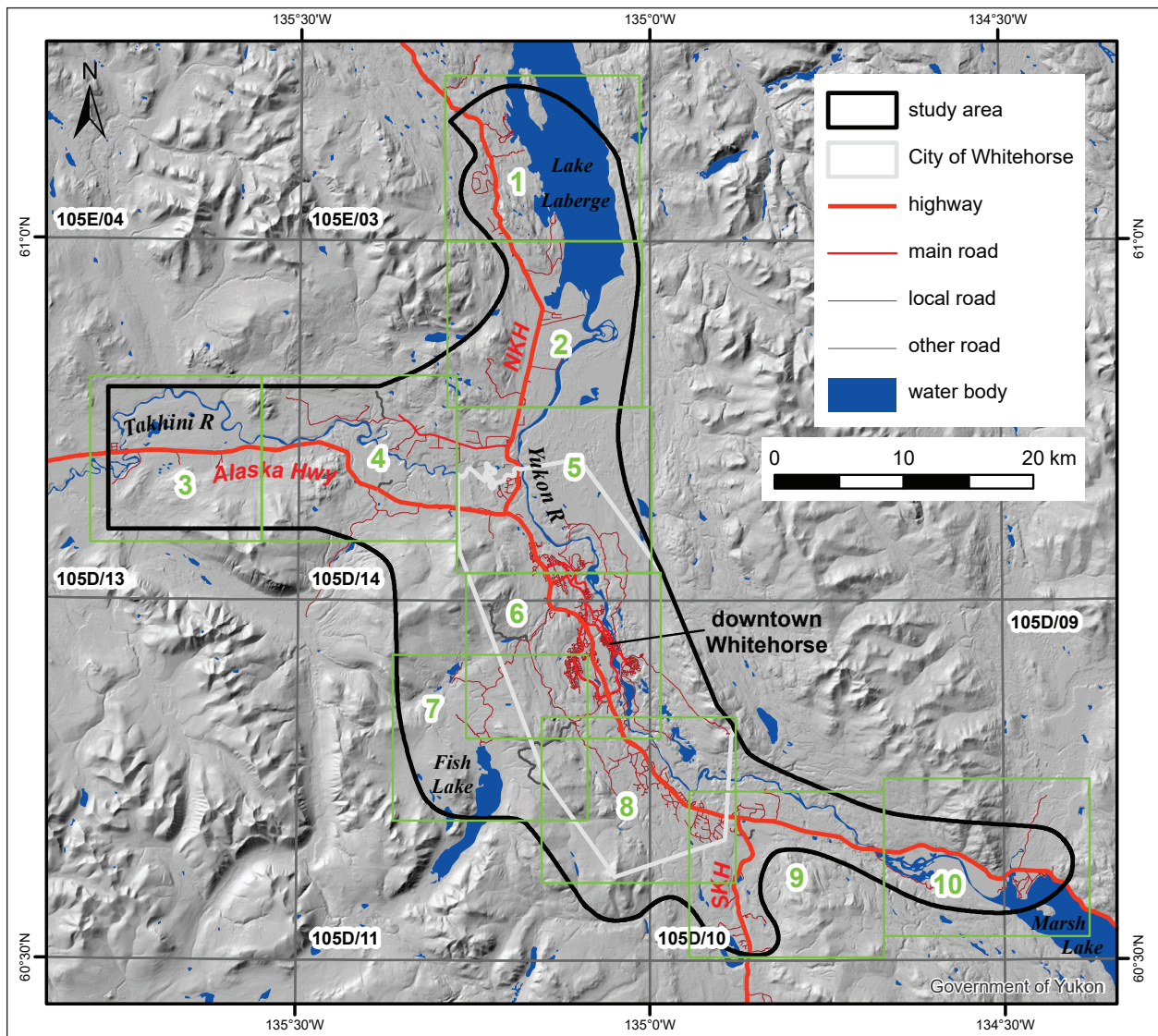
## Introduction

Remote predictive community-scale surficial geology mapping was completed for the greater Whitehorse area, through desktop interpretation of recent high-resolution imagery (primarily 2013–2019 lidar (Light Detection and Ranging) and 2007 air photos), and supported by field investigations carried out during the 2017–2021 field seasons. The nominal scale of mapping is 1:15 000, although some features were mapped at scales as large as 1:5000. This report provides background on the mapping methodology and classification system used, as well as some discussion of geohazards. The surficial geology is provided as a series of ten 1:15 000 scale map sheets in PDF format (Sheets 1 to 10; Fig. 1), and digitally in Esri geodatabase format (with standardized symbology files), as an accompaniment to this open file report. The map was also used to develop an aggregate potential model (Sheet 11), which can be used to help guide future exploration for gravel resources in the study area.

Geohazards that exist within the study area include landslides, radon gas, seismicity, permafrost and flooding. This report focusses on landslides as the primary geohazard, and includes a robust summary of the unprecedented landslide activity along the Whitehorse escarpment that occurred in early 2022. Recent and historical landslide features are also identified in the accompanying surficial geology map.

Landforms that indicate the presence of permafrost are likewise identified in the surficial geology map. Additionally, Yukon Geological Survey (YGS) collaborated with Yukon University Research Centre (YRC) from 2017 to 2021 to characterize permafrost in the region in detail. The results of this work were recently published by Roy et al. (2021). Their report also provides a summary of historical climate trends and future climate change projections for the Whitehorse area.

The project area (Fig. 1) includes the City of Whitehorse municipality, as well as surrounding areas that extend up to approximately 30 km outside the city limits where a variety of land-use pressures exist, such as agriculture and subdivision development. The boundaries of the study area were also selected to encompass lidar datasets available at the time of mapping. The mapping extends as far west as Takhini River subdivision in Ibex Valley, north to Deep Creek on Lake Laberge, east to Army Beach on Marsh Lake, and south to Cowley Lake. It also includes the Fish Lake and Grizzly Valley areas, as well as the Takhini Hot Springs Road.



**Figure 1.** Index map showing extent of the greater Whitehorse study area in relation to city limits, major water bodies, and road network (NKH = North Klondike Highway; SKH = South Klondike Highway). Accompanying 1:15 000 scale surficial geology map sheets outlined and numbered in green.

## Background setting

### Bedrock geology

The bedrock geology of the Whitehorse area has been mapped and described by Wheeler (1961), Hart and Radloff (1990), Hart (1997a,b,c,d), Hart and Hunt (1997), Colpron (2011), Bordet (2019), Bordet et al. (2019) and van Drecht et al. (2022). Gartner Lee (2003) also provides a concise summary of the bedrock found within city limits. Yukon Geological Survey (2022) maintains an online compilation map that is regularly updated and was used to generate the following simplified summary of the primary rock units shown in Figure 2. Bedrock outcrops are most common along ridge crests, hill tops, and valley sides. Overburden thicknesses of greater than 100 m are not uncommon within the Yukon and Takhini river valley bottoms.

The oldest rocks within the study area are found in the upper Paleozoic Takhini assemblage (uPT) to the west, which comprises mainly metamorphosed volcanic rocks and minor marble deposited approximately 323 million years ago (Ma). The Upper Triassic (229–200 Ma) Lewes River Group comprises a lower unit of volcanic rocks (the Povoas formation (uTrP)), and an upper unit of sedimentary rocks (the Aksala formation). The Aksala formation is subdivided into three members: the Casca (uTrAKC), Hancock (uTrAKT) and Mandanna (uTrAKK) members. The Casca member consists of clastic sedimentary rocks such as shale, siltstone, calcareous sandstone, and argillaceous limestone. The Hancock member consists of massive to thick-bedded limestone, which is easily viewed on Grey Mountain, and is described in detail by Yarnell *et al.* (1999). The Mandanna member comprises clastic rocks of green and red sandstone, pebble conglomerate, and mudstone, which are well exposed on Haeckel Hill, at the junction of the Alaska and South Klondike highways, and at the Takhini Hot Springs (described in detail by Long (2005)).

The Lower to Middle Jurassic (199–175 Ma) Laberge Group rocks were deposited in the Whitehorse trough during the early development of the Cordilleran mountain belt (Colpron *et al.*, 2015, 2022). These rocks are primarily found north of the Takhini Hot Springs Road and in the uplands west of the Old Alaska Highway. The prominent unit of the Laberge Group in the Whitehorse area is the Richthofen formation (JL1) comprising turbiditic sandstone, siltstone, mudstone and conglomerate. The Nordenskiöld member (JN) consists of khaki-green dacite crystal tuff and volcanoclastic sandstone dated at 188–183 Ma. These marine sedimentary units were folded, faulted and uplifted around 170–150 Ma (Heon *et al.*, 2004).

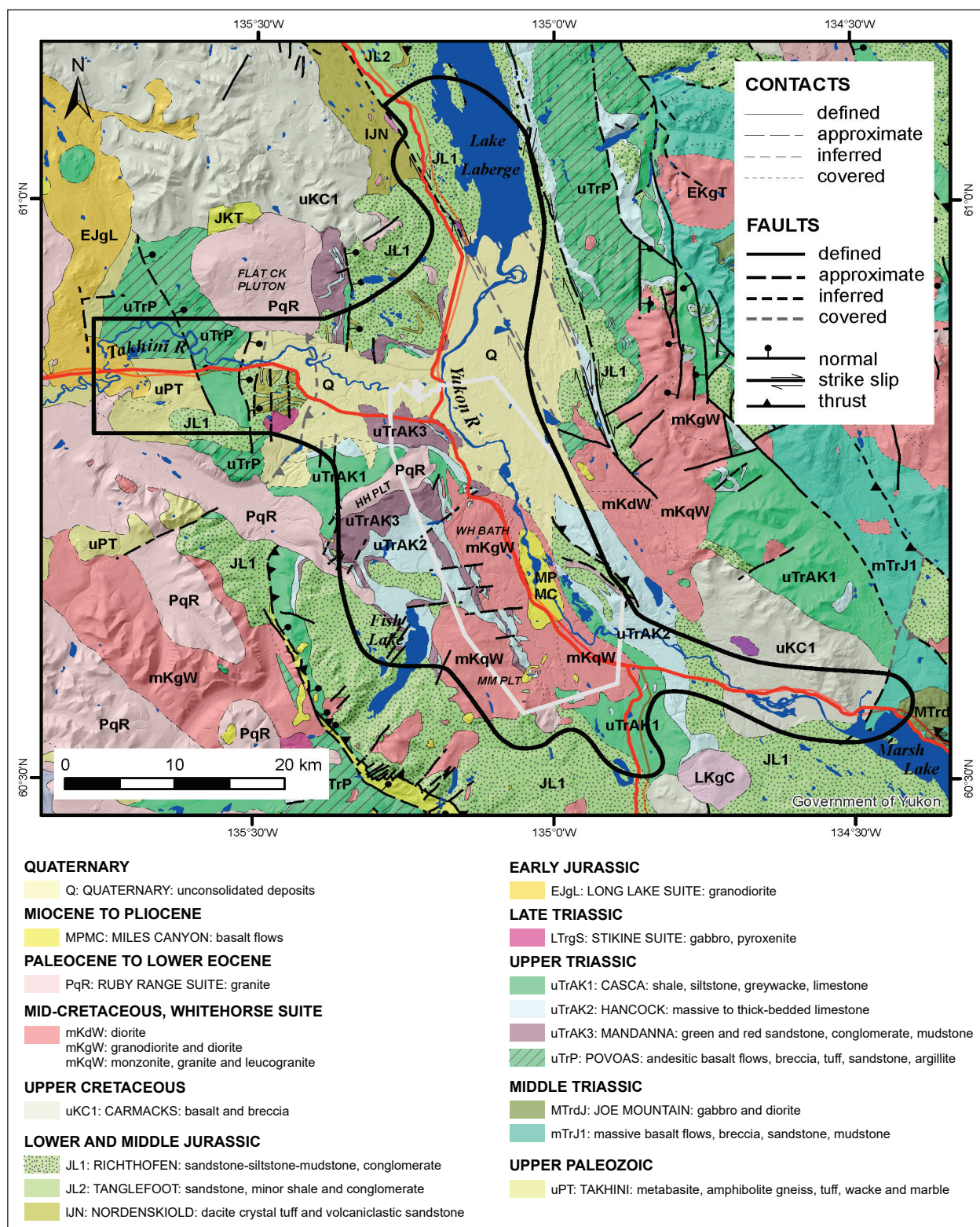
The area was then intruded by large granitic plutons in the mid-Cretaceous. The Whitehorse plutonic suite (112–105 Ma) includes the Whitehorse batholith (mKgW), which is largely composed of granodiorite and diorite, and the Mt. McIntyre pluton (mKqW), comprising quartz monzonite, granite and leucogranite. In surface exposures, these granitic rocks commonly weather and decompose into a veneer of unconsolidated coarse sand to pebble-sized grus; prominent examples occur along lower Fish Lake Road and at the south end of Ice Lake (located near the junction between the Alaska Highway and South Access Road). Several copper skarn deposits formed at the contact between these intrusions and the limestone of the Hancock member. The resultant Whitehorse Copper Belt, which was actively mined in the early 1900s and 1970s, is described in field guides by Héon and Hart (1998), Héon (2004) and Héon *et al.* (2004).

Upper Cretaceous (70–68 Ma) basalt of the Carmacks Group locally covers older units near Marsh Lake and west of Lake Laberge. A number of smaller granitic plutons of the Ruby Range suite (PqR) were intruded during the Paleocene (between 64–57 Ma), and include the Haeckel Hill and Flat Creek plutons.

In the upper Miocene, lava flows erupted several times between 8.9 and 3.2 Ma from a volcanic vent located on the north flank of Golden Horn Mountain (Hart and Villeneuve, 1999; Pearson *et al.*, 2001; Eberle *et al.*, 2019). The olivine-rich lava flowed from approximately Mary Lake to Riverdale subdivision, and cooled to form the Miles Canyon Basalt (MPMC), which is commonly columnar jointed (an indication that lava flows were subaerial). A sequence of basalt flows nearly 110 m thick was encountered in a water well on the south side of Riverdale (Gartner Lee, 2003).

Major faults in the area include the Braeburn strike-slip fault, and the Ibex thrust fault. The Braeburn fault trends in a northwest direction, extending from Grey Mountain, and following the South Klondike Highway to west of Lake Laberge. The north-south trending Ibex thrust fault is mapped west of Scout and Fish lakes. A series of parallel, east-west trending faults also occur throughout the Whitehorse Copper Belt. None of these faults have been recently active.





**Figure 2.** Simplified bedrock geology of the greater Whitehorse area (Yukon Geological Survey, 2022); see legend on following page. The study area is outlined by the heavy black line, and the City of Whitehorse boundary is outlined by the light grey line. WH BATH = Whitehorse Batholith; MM PLT = Mt. McIntyre Pluton; HH PLT = Haeckel Hill Pluton.

## Quaternary geology and landscape evolution

The landscape and glacial history of the Whitehorse area has been extensively described by many previous authors, most notably Mougeot GeoAnalysis (1997), Gartner Lee Ltd. (2003) and Bond (2004), and was summarized by the author in Roy et al. (2021) as follows:

The landforms and surficial materials within the Greater Whitehorse Area (GWA) are largely a product of the most recent (McConnell) ice age, and subsequent modification by fluvial and colluvial activity throughout the Holocene (the last 11 000 years). This section presents some key highlights of a very complex local landscape history, which is discussed and illustrated in detail by Bond (2004) and Mougeot GeoAnalysis (1997).

The McConnell (Late Wisconsinan) Glaciation occurred between ~24 000 and 11 000 years ago (Bond, 2004). At the maximum extent of this glaciation, ~18 000 years ago, the entire GWA was covered in ice at least 1350 m thick (Bond, 2004). At this time, ice flow was generally in a northwesterly direction, and was unobstructed by local topography. During deglaciation, the ice thinned and retreated to the southeast, punctuated by local standstills and topographically controlled readvances (Bond, 2004; Bond et al., 2005a–g). Cosmogenic radionuclide ( $^{10}\text{Be}$ ) surface exposure dating of large glacially transported boulders (erratics) indicate that the top of Mount McIntyre was ice-free by about 15 500 years ago, while the Raven's Ridge subdivision area (north of the city centre) was ice-free ~2000 years later (Menounos et al., 2017).

During early deglaciation (Cassiar Readvance phase), a lobe of ice readvanced northward down the Yukon River valley to the north end of Lake Laberge, where it deposited a large recessional moraine (Bond, 2004). As the ice later retreated to the south, Glacial Lake Laberge was impounded between this moraine and the ice front. The lake outlet gradually eroded through the moraine, causing lake levels to drop from a maximum elevation of about 716 m ~12 000 years ago, to 650 m ~10 600 years ago; it continued to drop throughout the Holocene to an elevation of 634 m ~3000 years ago (Horton, 2007).

During the Cassiar Readvance, another lobe of ice advanced up the Takhini River valley as far west as the village of Champagne (Bond, 2004) where it deposited a recessional moraine. This ice lobe dammed the Takhini River, while the St. Elias Lobe also dammed the Dezadeash River valley farther to the west. These two dams impounded Glacial Lake Champagne, which inundated much of the Kusawa Lake, Takhini River and Dezadeash River valleys. The lake rose to a maximum elevation of 854 m, with prominent stages at elevations of 765 m, and 725 m (Barnes, 1997; Gilbert and Desloges, 2005). The 746 m lake stage was controlled by an outlet draining northward through a divide located near Taye Lake, which drains into the headwaters of the Nordenskiöld River (Bond et al., 2005g). It has been speculated that Lake Champagne existed sometime between 12 500 and 10 500 years ago for a relatively short period of a few hundred years (Barnes, 1997), although others have argued that the lake drained as late as 7200 years ago based on the lack of older archeological sites in the valley (Heffner, 2008). Smaller glacial lakes also formed in the Ibex and Fish Lake valleys during this phase.

Once the ice fully retreated out of the Takhini Valley, Glacial Lake Champagne drained into Glacial Lake Laberge. A thick (often exceeding 50 m) sequence of fine-grained (fine sand, silt and clay) glaciolacustrine sediment settled out at the bottom of these glacial lakes, filling much of the Takhini and Yukon river valleys. Thicknesses in excess of 100 m are often reported in water well records in Takhini Valley, and a thickness greater than 300 m was logged in a well located near the Alaska Highway crossing of Takhini River (EBA, 2014). Ice-rich permafrost and thermokarst terrain is commonly associated with these fine-grained glaciolacustrine sediments. The sediments also constitute some of the most productive agricultural soil in the Whitehorse area. As Glacial Lake

Laberge gradually shrunk to its modern size, its southern shoreline migrated northward, and a thick (up to 4 m) blanket of well-sorted deltaic sand was deposited on top of the glaciolacustrine sediment. As lake levels continued to drop, dry deltaic sediments were exposed to extensive wind erosion, and a thin veneer of loess (wind-blown fine sand and silt) was deposited on the ground surface in many locations around Whitehorse. Extensive fields of sand dunes also formed north of the municipal sewage lagoons, and near the junction of Takhini Hot Springs Road and the North Klondike Highway. These dunes stabilized 9000 to 10 000 years ago as the boreal forest became the dominant vegetation cover in the valley bottoms (Wolfe et al., 2011).

Throughout the Holocene, the Takhini and Yukon rivers and smaller tributaries cut down through the glaciolacustrine sediments, creating the steep bluffs that are now found in these valley bottoms, (e.g., the Whitehorse airport escarpment). Extensive sedimentation occurred along the floodplains of both rivers during this time, and fluvial terraces (e.g., upon which Whitehorse and Riverdale are built) were formed as the base level continued to drop.

Till (or moraine) is a very widespread surficial material generally found above 700 m of elevation throughout the Whitehorse area. Till is sediment that has been transported directly by glacier ice, i.e., beneath, within, or on top of the glacier. The nature and composition of till can vary widely, but basal or lodgement till is one of the most common forms, which typically comprises a dense, poorly drained, matrix-supported diamicton, with a silty-sand matrix, and a large proportion of pebbles, cobbles and boulders. Basal till is commonly fluted or streamlined, indicating the direction of ice-flow. Thick blankets of till may be found in valley bottoms and lower slope positions. Middle to upper slope positions and ridge crests are generally mantled with thinner till veneers, which are modified by colluvial activity (downslope gravitational movement). Till found in recessional, lateral and stagnation moraines is typically less dense and coarser grained compared to basal till. During deglaciation, ice stagnation occurred several times, leaving behind a series of prominent recessional moraine ridges in Takhini Valley, (e.g., Stevens quarry).

Coarse-grained glaciofluvial sediments, primarily comprising sand and gravel, were deposited by glacial meltwater streams during deglaciation. Glaciofluvial plains, fans, terraces, and hummocky kame topography are particularly extensive near the subdivisions of Whitehorse Copper, Wolf Creek, and Cowley Creek. The hummocky Chadburn and Long Lake ice-contact kame and kettle complexes were also deposited during a period of ice stagnation as orphaned blocks of ice were buried and subsequently thawed. Glaciofluvial materials are generally coarse and well drained, and therefore are not usually associated with ice-rich permafrost.

Lateral meltwater channels (e.g., most notably along the lower east flanks of Mt. McIntyre, west and south of Grey Mountain, and in the Scout Lake area) are distinctive erosional features formed by glacial meltwater flowing along the margins of ice lobes. The channels typically support much smaller (underfit) contemporary streams and adjacent wetlands. Thick organic materials (fibric peaty material formed from decomposed vegetation fragments) generally accumulate in their floors. Organic veneers also commonly mantle north-facing slopes. These settings are commonly associated with permafrost due to the insulative capacity of the organic materials.

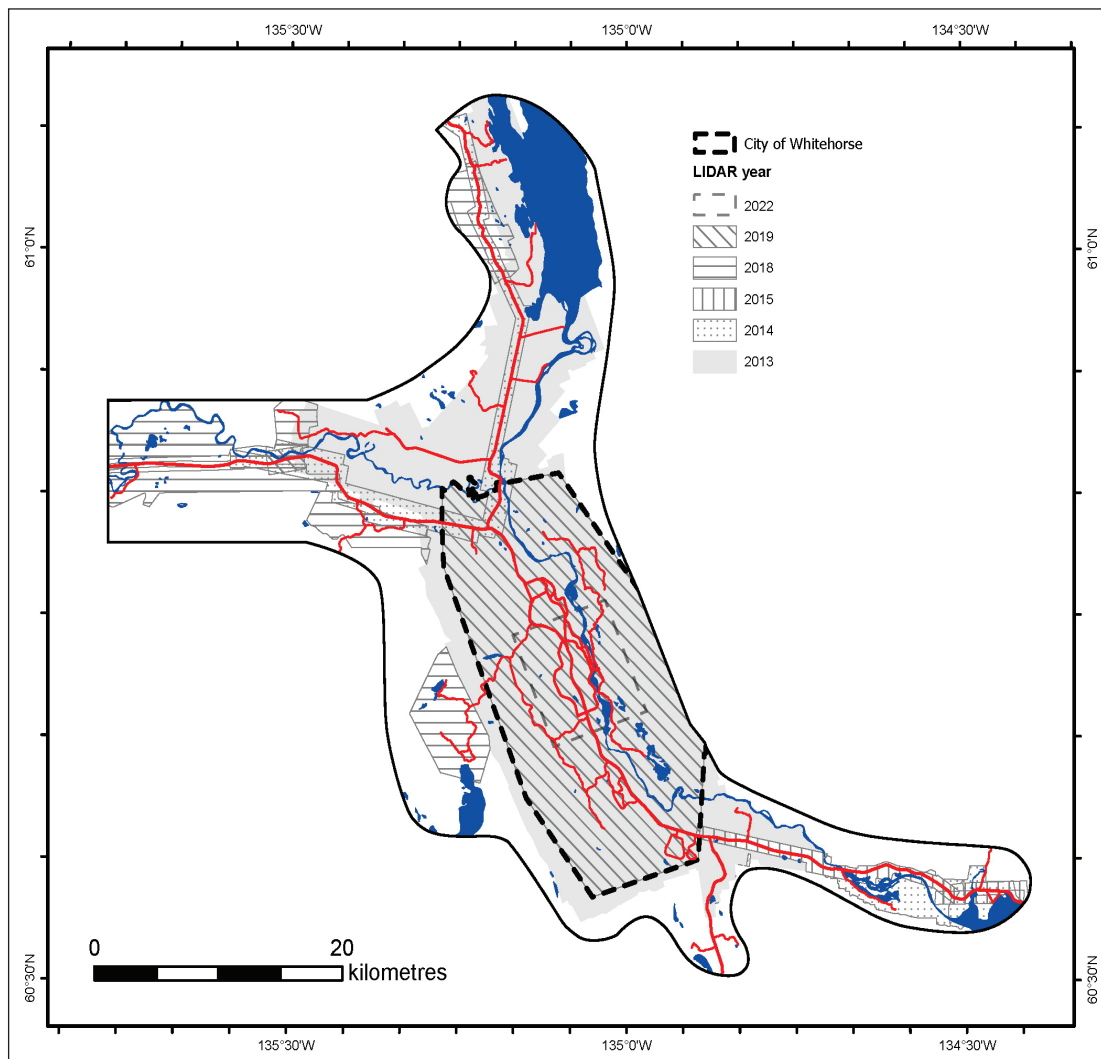
## Data sources and methods

### Field investigations

More than 400 sites were visited and described in the field to characterize representative map units and landforms and verify desktop interpretations. Field investigations generally consisted of manually digging soil pits up to one metre deep, or examining sediment exposed in road cuts, excavations, landslide escarpments, and stream cutbanks. At each site, landform surface expression and sedimentological characteristics of exposed stratigraphic units were described and documented with photos. Geophysical surveys, drone surveys, frost probing, and shallow drilling were also completed at selected sites.

### Lidar

Geological features and waterbody shorelines were digitized from bare earth lidar hillshade models (derived from one metre-grid digital terrain models (DTMs)) for approximately two thirds of the study area (Fig. 3). The lidar data surveys that were used range in age from 2013 to 2022 (Fig. 3 and Table 1), with mean point cloud densities on the order of approximately 10 pts/m<sup>2</sup>. The 2022 lidar data were also used to map landslides along the airport escarpment.



**Figure 3.** Index map of lidar surveys used for mapping.

**Table 1.** Summary of lidar surveys and air photos used for mapping.

<b>Lidar</b>		
<b>Date</b>	<b>Area</b>	<b>Mean Point Cloud Density (pts/m<sup>2</sup>)</b>
2013-07-19	City of Whitehorse	10
2013-2015	Greater Whitehorse, Hot Springs Road, Lake Laberge, Golden Horn	
2014	Marsh Lake	
2018-09-22	Fish Lake	
2018-09-22	Ibex Valley/Old AK Hwy	
2018-09-26	Hot Springs Road	
2018-09-19 to 29	Grizzly Valley	10.1
2019-09-28	Ibex Valley	9.93
2019-09-29	City of Whitehorse	10.11 (3.09 BE)
2022-06-19	Whitehorse airport	9-60
<b>Air Photos</b>		
<b>Year</b>	<b>Roll Number</b>	<b>Scale</b>
1946	A10552, A10553, A10557, A10560, A10563, A10565	1:30 000
2007	A28542-A28546 (flown mid July to mid August 2007)	1:40 000

## **Aerial photographs**

Aerial photographs and high-resolution satellite imagery were used as a complementary data source for geological interpretation, particularly where no lidar data were available. The air photos utilized were primarily of 2007 vintage and originally printed at 1:40 000 scale. However, high-resolution (2012 dpi) scans of the original air photo negatives permitted features to be accurately digitized at up to 1:10 000 scale. Seventy-five 1946 air photo scans (1:30 000 scale) were also acquired to allow interpretation of surficial materials underlying developed areas. The scanned air photos were aerial triangulated to fit the 1:50 000 scale CanVec (Natural Resources Canada) topographic base data. Photogrammetry models were produced to support soft copy stereoscopic analysis in DAT/EM Summit Evolution Lite software, which was linked to an Esri ArcMap platform for digitizing tools.

## **Borehole data**

The Yukon water well registry (Environment Yukon, 2022) was an invaluable resource for determining the thickness of overburden or depth to bedrock, and the subsurface stratigraphy. More than 1200 water wells are currently included in the registry within the study area; more than 900 of these provide some indication of depth to bedrock, and more than 800 have original well logs available online. More than four hundred water wells intersected bedrock and therefore provide an absolute overburden thickness, whereas the depth of drilling for remaining wells determined the minimum overburden thickness. In the “surficial\_points” layer of the appended surficial geology geodatabase, depth to bedrock for selected water wells is recorded in the OB\_THICK\_M field. Detailed well logs for more than 400 water wells were also reviewed to inform surficial geology interpretations; summary stratigraphy for these holes may be viewed in the COMMENTS field of the “surficial\_points” layer in the appended surficial geology geodatabase. Original well logs may be viewed by hyperlinking to the URLs in the SOURCE field.

The Yukon Permafrost Database (Lipovsky et al., 2022) was also a very helpful resource for confirming map unit interpretations. The database contains geotechnical data and soil descriptions for 2794 boreholes located within the study area. Tetra Tech EBA originally compiled 2361 of these for geotechnical investigations they conducted prior to 2010. Most of the remaining boreholes were derived from the Alaska Highway borehole database, which was compiled from Yukon Highways and Public Works borehole investigations conducted from the 1970s to 1990s.

## **Surficial geology and soil survey maps**

Different parts of the Greater Whitehorse were previously mapped (Table 2) at different scales using a variety of surficial geology and soil mapping classification schemes. These maps provided a wealth of baseline information that was reviewed during the interpretation of the new mapping.

## **Surficial geology mapping classification system**

Surficial geology polygon map units were classified using the Terrain Classification System for British Columbia (Howes and Kenk, 1997) with minor modifications developed for Yukon Geological Survey's mapping standards (Yukon Geological Survey, 2020) to include a wider variety of permafrost features and age classifications.

A sample polygon map label or terrain unit is shown in Figure 4. Surficial material forms the core of the polygon map labels and is represented by the first single upper case letter in each terrain unit. Up to three textural codes are written in lower case to the left of each surficial material (listed in order of decreasing dominance), and up to three surface expression codes are written in lower case to the right. An upper case activity qualifier (A = active; I = inactive) may be shown immediately following the surficial material. Alternatively, the glacial qualifier "G" may be written immediately following the surficial material to indicate materials that were deposited in close proximity to glaciers. Age is indicated by a capital letter that follows the surface expression, but precedes any geomorphological process modifiers. Up to three geomorphological processes (capital letters) and subclasses (lower case letters) always follow a dash ("-") symbol. Detailed definitions for the polygon map label codes are provided in subsequent sections.

Up to four terrain units may be combined in a complex polygon map label if they could not be differentiated at the scale of mapping. Each terrain unit is separated by a delimiter that either indicates relative proportions between the components (":", "/", "//") or stratigraphic relationships ("^").

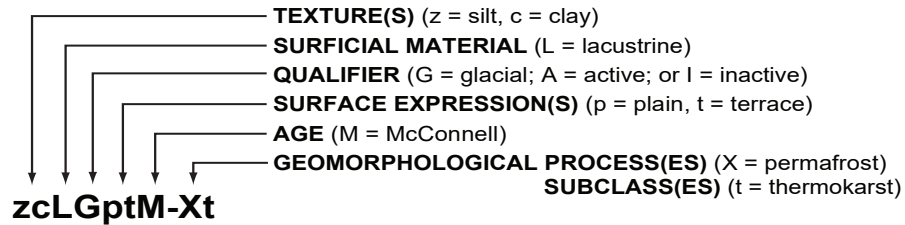
## **Surficial materials**

### ***Anthropogenic (A)***

Anthropogenic materials are artificial or geological materials that have been deposited and/or modified by human activities such that their original physical properties have been significantly altered. This includes mine tailings, landfill materials, and earthen structures such as dams, berms, dykes, sewage lagoons, and road and building pads.

**Table 2.** Summary of previous surficial geology and soil survey maps reviewed during mapping.

Year	Scale	Author	Name	Map No
1978	1:100 000	Klassen, R.W.	Surficial Geology, Takhini River, Yukon Territory	GSC OF539 (Map 1)
1982a	1:100 000	Morison, S., McKenna, K. and Davies, S.	105D NE Surficial Geology and Soils (Southern Lakes Project)	unpublished (YG)
1982b	1:100 000	Morison, S., McKenna, K. and Davies, S.	105D NW Surficial Geology and Soils (Southern Lakes Project)	unpublished (YG)
1982c	1:100 000	Morison, S., McKenna, K. and Davies, S.	105D SE Surficial Geology and Soils (Southern Lakes Project)	unpublished (YG)
1982d	1:100 000	Morison, S., McKenna, K. and Davies, S.	105D SW Surficial Geology and Soils (Southern Lakes Project)	unpublished (YG)
1987	1:250 000	Klassen, R.W. and Morison, S.R.	Surficial geology, Laberge, Yukon Territory	GSC Map 8-1985
1991	1:250 000	Morison, S.R. and Klassen, R.W.	Surficial geology, Whitehorse, Yukon Territory	GSC Map 12-1990
1997	1:20 000	Mougeot, C.M.	Soil, terrain and wetland survey, City of Whitehorse	unpublished (City of Whitehorse)
1998	1:40 000	Mougeot, C.M.	Soil and terrain features of the Yukon River corridor	unpublished (City of Whitehorse)
1998	1:30 000	Mougeot, C.M. and Smith, C.A.S.	Terrain and surficial geology of the City of Whitehorse	unpublished (City of Whitehorse)
1999	1:30 000	Mougeot, C.M. and Smith, C.A.S.	Soils of the City of Whitehorse, Yukon Territory	unpublished (City of Whitehorse)
2005	1:50 000	Bond, J.D., Morison, S. and McKenna, K.	Surficial Geology of Carcross	YGS GM2005-2
2005	1:50 000	Bond, J.D., Morison, S. and McKenna, K.	Surficial Geology of Fenwick Creek	YGS GM2005-3
2005	1:50 000	Bond, J.D., Morison, S. and McKenna, K.	Surficial Geology of Alligator Lake	YGS GM2005-4
2005	1:50 000	Bond, J.D., Morison, S. and McKenna, K.	Surficial Geology of Robinson	YGS GM2005-5
2005	1:50 000	Bond, J.D., Morison, S. and McKenna, K.	Surficial Geology of MacRae	YGS GM2005-6
2005	1:50 000	Bond, J.D., Morison, S. and McKenna, K.	Surficial Geology of Whitehorse	YGS GM2005-7
2005	1:50 000	Bond, J.D., Morison, S. and McKenna, K.	Surficial Geology of Upper Laberge	YGS GM2005-8
<b>Agriculture Canada Soil Survey (Report No. 2)</b>				
1992	1:20 000	Mougeot, C.M., and Smith, C.A.S.	Soils of the Whitehorse area, Takhini Valley	west sheet
1992	1:20 000	Mougeot, C.M., and Smith, C.A.S.	Soils of the Whitehorse area, Takhini Valley	central sheet
1992	1:20 000	Mougeot, C.M., and Smith, C.A.S.	Soils of the Whitehorse area, Takhini Valley	east sheet
1994	1:20 000	Mougeot, C.M., and Smith, C.A.S.	Soils of the Whitehorse area, Carcross Valley	north sheet
1994	1:20 000	Mougeot, C.M., and Smith, C.A.S.	Soils of the Whitehorse area, Carcross Valley	south sheet



TEXTURE	
<i>Specific clastic textures</i>	
a	blocks (>256 mm, angular)
b	boulders (>256 mm, rounded)
k	cobble (64-256 mm, rounded)
p	pebbles (2-64 mm, rounded)
s	sand (0.062 - 2 mm)
z	silt (0.002 - 0.062 mm)
c	clay (<0.002 mm)
<i>Grouped clastic textures</i>	
d	mixed fragments (>2 mm, rounded and angular)
x	angular fragments (>2 mm, mix of r & a)
g	gravel (>2 mm, rounded, mix of b, k, p)
r	rubble (2-256 mm, angular particles)
m	mud (mix of silt and clay)
y	shells (shells or shell fragments)
n	salt (evaporite crystals)
<i>Organic terms</i>	
e	fibric organic (poorly decomposed)
u	mesic organic (intermediate decomposition)

GEOMORPHOLOGICAL PROCESS	
<i>Erosional processes</i>	
-V	gully erosion
<i>Fluvial and hydrological processes</i>	
-M	meandering floodplain
-U	inundation
<i>Mass movement processes</i>	
-F	slow landslide
-R	rapid landslide
-L	undifferentiated landslide
<i>Periglacial processes</i>	
-N	nivation
-S	solifluction
-X	permafrost
<i>Deglacial processes</i>	
-E	channeled by glacial meltwater
-H	kettled
-T	ice-contact

SURFICIAL MATERIAL	
A	Anthropogenic
C	Colluvium
E	Eolian
F	Fluvial
FA	Active Floodplain
FG	Glaciofluvial
H	Water body
L	Lacustrine
LG	Glaciolacustrine
M	Morainal (till)
O	Organic
R	Bedrock

SURFACE EXPRESSION	
a	apron
b	blanket (>1m thick)
d	depression(s)
f	fan(s)
h	hummock(s)
l	delta
m	rolling
p	plain
r	ridge(s)
t	terrace(s)
u	undulating
v	vener (0.1 - 1 m thick)
w	mantle of variable thickness

MASS MOVEMENT PROCESS SUBCLASSES (follows -F, -L or -R)	
"	initiation zone
<i>Slow mass movement (follows -F)</i>	
c	soil creep
g	rock creep
k	tension cracks
p	lateral spread in bedrock
j	lateral spread in surficial material
<i>Rapid mass movement (follows -R)</i>	
b	rockfall
d	debris flow
f	debris fall
t	debris torrent
<i>Slow or rapid mass movement (follows -F, -L or -R)</i>	
e	earthflow
m	slump – in bedrock
u	slump – in surficial material
x	slump – earthflow
s	debris slide
r	rockslide
<b>PERMAFROST PROCESS SUBCLASSES (follows -X)</b>	
f	thaw flow slides
p	permafrost mounds (lithalsa, palsa, peat plateau)
t	thermokarst subsidence
<b>HYDROLOGICAL PROCESS SUBCLASSES (follows -U)</b>	
b	beaver dams

COMPOSITE SYMBOL DELIMITERS	
.	terrain unit(s) on either side of the symbol are of approximately equal proportion.
/	terrain unit(s) before symbol is more extensive than the following one(s). (Also denotes partial/discontinuous cover if located at front of label.)
//	terrain unit(s) before symbol is much more extensive than the following one(s).
\	terrain unit(s) before the symbol stratigraphically overlies the following one(s).

Figure 4. Summary of polygon map label codes used for mapping.



## **Organic (O)**

Organic deposits consist of at least 30% organic matter by weight, resulting from the accumulation of vegetative matter, primarily in wetlands. They are most commonly found at the surface above mineral soil and comprise partially decomposed fibrous peat with recognizable remains of moss, shrubs, sedges and fine roots. Surface organic veneers (Ov) up to 30 cm thick are widespread throughout the study area and are generally unmapped. Thicker surface blankets (Ob; >1 m thick) or plains (Op) are most common in valley bottoms in low-lying, poorly drained wetland areas (Fig. 5). Organic material is very effective at insulating the ground in summer, and it is strongly associated with near-surface, ice-rich permafrost.

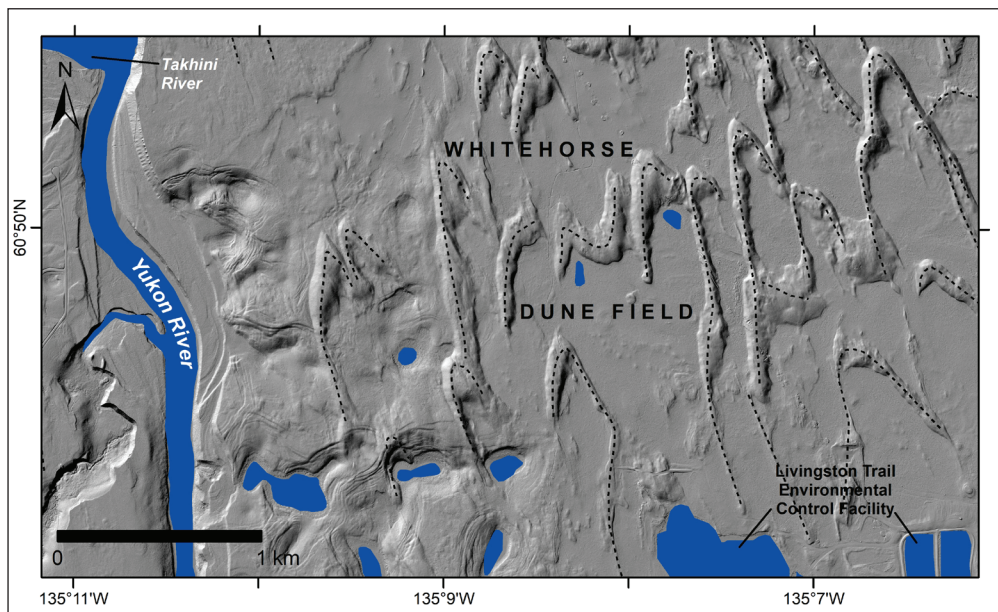


**Figure 5. (a)** Thick organic material (peat) and **(b)** associated wetland vegetation near Hillcrest subdivision (20PL021; August 4, 2020). The frost table was encountered at a depth of 35 cm at this location, which is likely very close to the top of permafrost (note white patches of ice at bottom of soil pit).

## **Eolian (E)**

Eolian materials are sediments that have been transported and deposited directly by wind. They are generally sourced from areas where an abundance of fine-grained sediment was exposed at the surface, such as glacial meltwater floodplains and drained glacial lakebeds.

A thin veneer of loess comprising silt and fine sand is commonly found near the ground surface in the Whitehorse area, but was generally not mapped. Thick blankets (Eb) and dunes (Er) of well-sorted eolian sand are found in the Whitehorse dune field, north of the city's Livingstone Trail sewage lagoons (Fig. 6), as well as in other localized areas (Fig. 7). The northwest-trending parabolic shape of the dunes indicates that the dominant paleo-wind direction was toward the northwest, likely draining katabatically off the lobe of ice retreating from Yukon River valley. Younger eolian deposits include small cliff-top sand dunes above large, recently active cutbanks along the Yukon and Takhini rivers, and beach dunes marking relict lake shorelines (e.g., Fox Creek, Shallow Bay, Swan Lake and Army Beach areas).



**Figure 6.** Lidar hillshade image clearly shows relict parabolic sand dunes in the Whitehorse dune field. Dashed lines trace the crest of the dunes, many of which are up to 1 km long and 20 m tall.



**Figure 7.** Sand dunes exposed along road cut near North Klondike Highway near Takhini Hot Springs Road (19PL027).

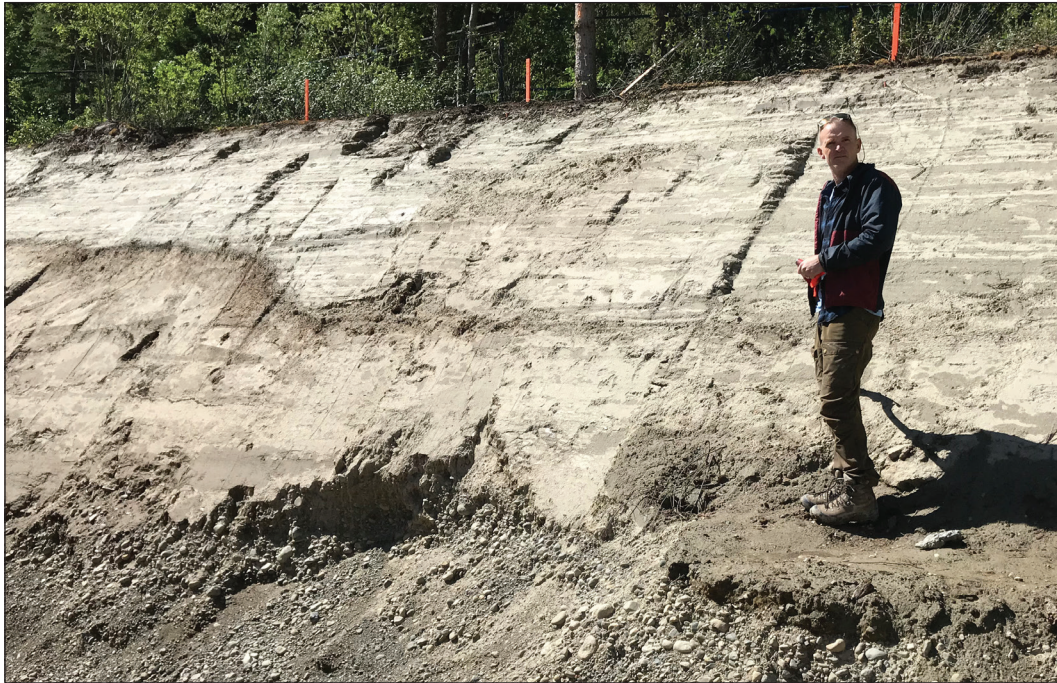
### ***Colluvium (C)***

Colluvium is material that was transported and deposited by downslope, gravity-driven mass movement processes such as creep, landslides and snow avalanches. The texture and composition of colluvium varies widely and depends on the transport mechanism, distance transported, and source parent material. Colluvial materials deposited by rapid mass movement processes, such as rock falls, debris flows, and avalanches, are typically found on steep to moderate slopes. Conversely, colluvium deposited by slower processes such as creep and seepage, occurs on more gentle to moderate slopes. Colluvium is commonly crudely stratified parallel to the slope angle, and may incorporate layers or fragments of organic material (Fig. 8).

Colluvial veneers (Cv) and blankets (Cb) are widespread on hillslopes throughout the study area, and commonly overlie till and/or bedrock. Thinner (<1 m) colluvial veneers are found on steeper upper slopes, while thicker (>1 m) blankets are found on gentler, mid to lower slopes. Colluvial fans (Cf) and aprons (Ca; complexes of laterally coalescing fans) commonly occur in slope toe positions (Fig. 9).



**Figure 8.** Fine-grained colluvium exposed on the Whitehorse escarpment on the south lateral margin of the 2022 Drury Street landslide initiation zone (J. Bond photo). Note buried organic horizon (arrow) and bedding structure parallel to the slope angle.



**Figure 9.** Apron of fine-grained colluvium (~2 m thick) exposed above fluvial sand and gravel in a foundation excavation, at the base of the Whitehorse escarpment near Main Street (18PL004b). Colluvial fans and aprons along the toe of the escarpment are generally comprised of similar material, which has accumulated from successive mud flow and landslide events.

## **Fluvial (F)**

Fluvial sediments (or alluvium) are transported and deposited by modern streams and rivers and are found in floodplain, terrace and fan landforms. They typically consist of stratified sand and gravel that is moderately to well sorted with subrounded to rounded clasts, and minor silt and organic deposits. The most extensive fluvial materials in the study area are associated with the Yukon and Takhini rivers. Finer grained sediments (silt to fine sand) and organic materials commonly occur in the floodplains of smaller tributaries.

Floodplains are considered active (FAp) where subject to ongoing or periodic reworking and inundation by flooding; these generally include bars that are unvegetated or sparsely vegetated with grass and/or shrubs (Fig. 10). Inactive floodplains (Fp) occur close to modern river levels and are generally forested, whereas terraces (Ft; Fig. 11) are older floodplain surfaces that have been incised following a base level change, leaving a sharp escarpment along one side. Fluvial fans (Ff) occur at the mouths of steeper drainages where flows become unconfined upon entering a higher-order or lower-gradient valley bottom. They typically comprise coarser and more poorly sorted material that may be interstratified with colluvial deposits. They are also subject to avulsions, when a sudden change occurs in the course of a stream channel.



**Figure 10.** Fluvial terrace sand and gravel (gsFt) exposed in a bank of the Yukon River in Riverdale subdivision. Shrubby gravel bar on opposite side of the river is considered part of the active floodplain (gsFAp). Note undercutting of bank occurring on outside of river bend.

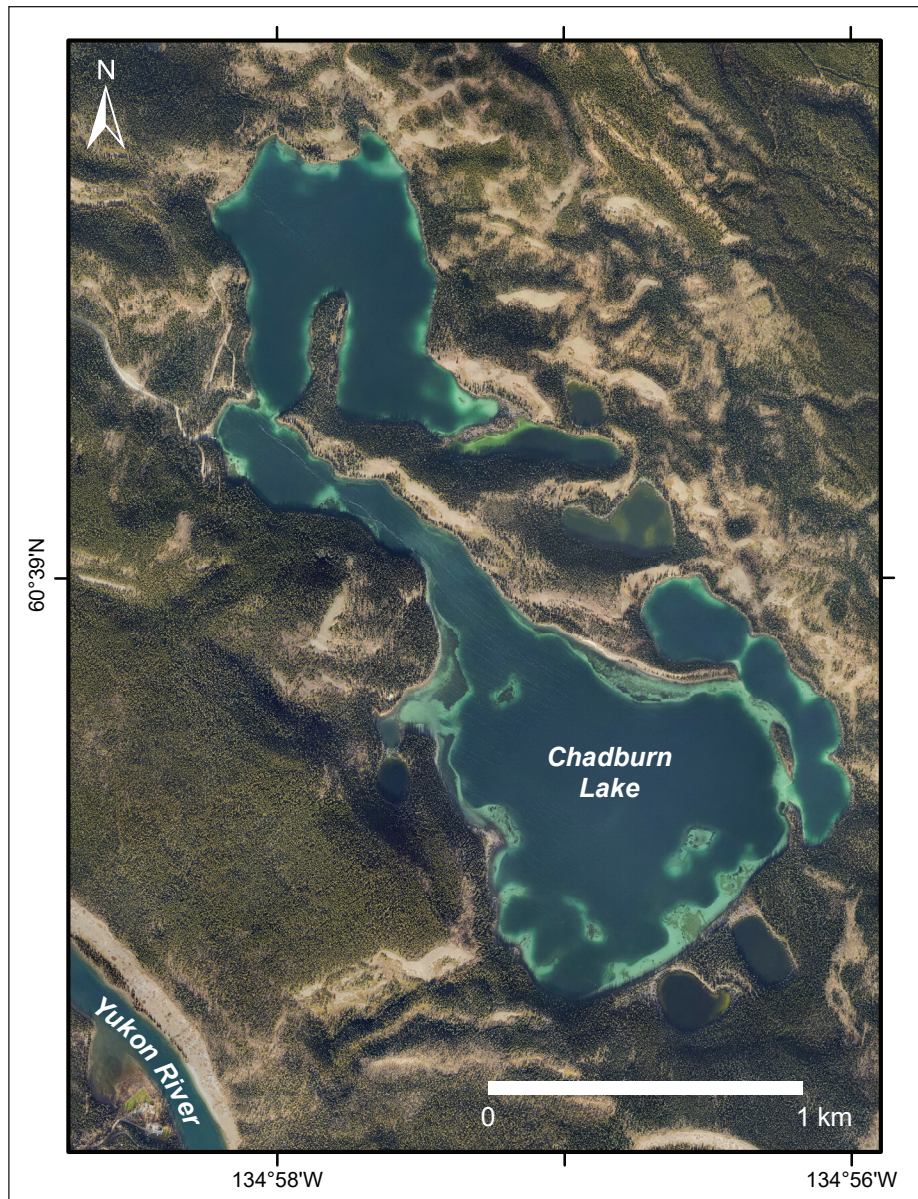


**Figure 11.** Fluvial sand and gravel exposed in infrastructure excavation near Wheeler St. and 6th Ave. This material underlies much of downtown Whitehorse, which is built on a terrace of the Yukon River (gsFt).

### **Lacustrine (L)**

Lacustrine sediments are deposited in modern (non-glacial) lakes, and generally consist of fine-grained sand, silt and clay.

Marl (yL) is a distinctive light-coloured, calcareous, lacustrine sediment that commonly accumulates on the bottom of shallow lakes located near limestone bedrock, and often gives shallow lakes a turquoise colour (Fig. 12). Marl primarily consists of calcium carbonate that was dissolved in groundwater and settled on the lake bottom as it biochemically precipitated out of solution (Vreeken, 1981). It also often contains abundant mollusc shells.



**Figure 12.** The turquoise colour in shallow portions of Chadburn Lake are due to marl deposits on the lakebed. The chaotic (hummocky, ridged and kettled; gsFGhrd-HT) nature of the surrounding terrain is the result of glacier ice stagnation in the area. 2019 orthophoto background.

### ***Glaciolacustrine (LG)***

Glaciolacustrine sediments are deposited in lakes that form on, in, under, or beside a glacier. While the nature of glaciolacustrine sediments can vary somewhat (Brideau et al., 2011), they most commonly consist of horizontally laminated fine sand, silt and clay (Figs. 13, 14 and 15) that settled out of suspension onto the lake bottoms, with rare coarse fragments (dropstones) fallen from ice bergs. Sandier cross-bedded and rippled sediments were likely deposited by turbidity flows and currents in shallower near-shore and deltaic environments. Extensive glaciolacustrine sediments, commonly up to 100 m thick, were deposited within the Yukon and Takhini river valleys in glacial lakes Champagne and Laberge. Abundant relict shorelines are also associated with these glacial lakes. The shorelines are generally erosional features cut into the surrounding slopes; however, some may also comprise sand and gravel beach and sand dune deposits.



**Figure 13.** Glaciolacustrine sediments exposed in the Whitehorse escarpment above Hawkins Street (20MK018a) primarily consist of horizontally bedded silt. Note person circled for scale.



**Figure 14.** Glaciolacustrine sand exposed in a quarry near the Yukon Wildlife Preserve (18PL075).



**Figure 15.** Glaciolacustrine sediments exposed in a roadcut along Takhini River Road (18PL074) consist of horizontally laminated layers of silt (thicker, lighter coloured layers) and clay (thinner, darker coloured layers up to approximately 5 cm thick). These sediments are easily eroded and are subject to gullying and piping in this area.

Mougeot (1994) investigated the properties of clay from various glaciolacustrine deposits in the Whitehorse area and evaluated their suitability for industrial (e.g., ceramic) use. The Takhini and McClintock river valleys were identified as the most promising areas to find favourable clay deposits.

### **Glaciofluvial (FG)**

Glaciofluvial materials are deposited directly by glacial meltwater and form above, in, below, or adjacent to a glacier. Glaciofluvial deposits generally consist of well-drained, moderately to well-sorted, stratified sand and gravel (Fig. 16), but exact characteristics vary locally depending on transport distance and setting. Their high sand and gravel content makes glaciofluvial materials an optimal source for aggregate.

Glaciofluvial deposits occur in a variety of landforms, including outwash plains (FGp), terraces (FGt), fans (FGf), deltas (FGI), and ice contact complexes (-T) that commonly contain kames (FGh), eskers (FGr), and kettled terrain (-H) with depressions (FGd). The most prominent ice-contact complex in the area occurs in the Chadburn Lake area (see Fig. 12), where large blocks of stranded glacier ice were buried by glaciofluvial outwash, and then depressions (kettles) formed when the ice blocks eventually melted. Another distinctive glaciofluvial feature in the study area is the mantle of deltaic glaciofluvial sand (sFGI; Fig. 17) that caps the Whitehorse escarpment glaciolacustrine sediments.

The presence of glacial meltwater channels is indicated by the geomorphological process symbol “-E”. These erosional glaciofluvial landforms are abundant within the study area. Where they occur on valley sides, they mark the lateral extent of glaciers at a certain point in time. As the glaciers thinned and retreated, subparallel flights of lateral meltwater channels were formed, prominent examples of which occur in the Scout Lake area, and on the southern flanks of Grey Mountain. Larger-scale subglacial and proglacial meltwater channels also occur in valley bottoms, where they now host underfit modern streams, such as McIntyre Creek (Fig. 18).



**Figure 16.** Stratified and cross-bedded glaciofluvial gravel exposed in a pit north of Haeckel Hill (19PL043a).



**Figure 17.** Approximately 5 m of well-sorted deltaic (glaciofluvial) sand exposed in a foundation excavation in the Takhini North subdivision (20PL038).



**Figure 18.** Upper McIntyre Creek is an underfit stream that occupies the floor of a large meltwater channel. View is to the south, with Copper Ridge subdivision in the background.



### **Morainal (M)**

Morainal (till) materials are deposited by either primary glacial processes such as lodgement, deformation and ablation (melt-out), or secondary glacial processes caused by gravity and water (e.g., flow tills). Till generally consists of a diamict made up of poorly sorted, subangular to subrounded pebble to boulder sized clasts of mixed rock types in a sandy-mud matrix (i.e., texture “dsm”; Fig. 19).

Lodgement (or basal) till typically has an even (Mv and Mb) or rolling/streamlined (Mm) surface expression. Ablation (or melt-out) till generally has a hummocky (Mh) and/or kettled (pitted; M-H) surface expression, with a looser or sandier matrix. On valley sides, till is commonly modified by colluviation, as indicated by slope parallel structures within the till.

Moraine ridges (Mr) deposited along the flanks (lateral moraines) or toes (recessional moraines) of retreating glaciers are present in many locations throughout the map area, mostly west of the Yukon River and south of the Takhini River. Crevasse fillings are also a common occurrence, and stand out on lidar imagery as low (<5 m high) subparallel ridges oriented perpendicular to ice flow direction (e.g., Squatters Road area, 2 km west of Miles Canyon).



**Figure 19.** Thick exposure of lodgement till diamict near the Old Alaska Highway (19PL021). Note the wide range of clast sizes from boulders to pebbles, which are supported in a dense, fine-grained matrix.

## **Bedrock (R)**

Bedrock outcrops are most common in upland areas on summits and ridge tops, and along valley sides throughout the map area. Bedrock is also exposed in valley bottom environments, where it has been carved or scoured by ice (Figs. 20 and 21) and/or concentrated subglacial meltwater (e.g., rock gardens near the Alaska Highway and South Access Road junction) or where lava flows have been exposed by fluvial erosion (e.g., Miles Canyon basalts exposed in the Yukon River at Miles Canyon). In some locations, granitic rocks have weathered and decomposed into a surface veneer of coarse sand to pebble-sized grus (e.g., lower Fish Lake Road and the south end of Ice Lake, which is located approximately one kilometre northwest of the Alaska Highway and South Access Road junction). Depth to bedrock is highly variable and overburden thicknesses in excess of 100 m are not uncommon in the valley bottoms.



**Figure 20.** Sandstone outcrop (Mandanna member of the Lewes River Group Aksala formation) near Porter Creek Secondary School (20PL026a). Crag and tail streamlined morphology and striations on the rock surface indicate that the ice-flow direction was northwesterly. Abundant limestone outcrops exposed on Grey Mountain in background.



**Figure 21.** Scoured granodiorite with crosscutting dikes exposed after stripping thin overburden along the Hamilton Boulevard extension.

## Texture

Texture refers to the size, shape and sorting of particles in clastic sediments, and the proportion and degree of decomposition of plant fibre in organic-rich material (Table 3). Texture is indicated by up to three lower case letters, placed immediately before the surficial material designator, and listed in order of decreasing abundance (in contrast to the British Columbia terrain classification system).

**Table 3.** Texture codes and definitions used in the appended greater Whitehorse surficial geology map unit classifications. Starred items highlight additions/deviations from the BC terrain classification system.

<b>Specific clastic textures</b>		
a	blocks	angular particles >256 mm in size
b	boulders	rounded particles >256 mm in size
k	cobbles	rounded particles >64–256 mm in size
p	pebbles	rounded particles >2–64 mm in size
s	sand	particles between >0.0625 and 2 mm in size
z	silt	particles 2 µm (0.002 mm)–0.0625 mm in size
c	clay	particles ≤2 µm (0.002 mm) in size
<b>Common clastic textural groupings</b>		
d	mixed fragments	a mixture of rounded and angular particles >2 mm in size
x	angular fragments	a mixture of angular fragments >2 mm in size ( <i>i.e.</i> , a mixture of blocks and rubble)
g	gravel	a mixture of two or more size ranges of rounded particles >2 mm in size ( <i>e.g.</i> , a mixture of boulders, cobbles and pebbles); may include interstitial sand
r	rubble	angular particles between 2 and 256 mm; may include interstitial sand
m	mud	a mixture of silt and clay; may also contain a minor fraction of fine sand
y	shells or marl	a sediment consisting dominantly of shell fragments and/or calcium carbonate precipitates
n	salt*	saline soils with evaporitic salt crystals on the ground surface
<b>Organic terms</b>		
e	fibric	the least decomposed of all organic materials; contains 40% or more of well-preserved fibre that can be identified as to botanical origin upon rubbing
u	mesic	organic material at a stage of decomposition intermediate between fibric and humic
h	humic	organic material at an advanced stage of decomposition; it has the lowest amount of fibre, the highest bulk density, and the lowest saturated water-holding capacity of the organic materials; fibres that remain after rubbing constitute less than 10% of the volume of the material

## Surface expression

Surface expression refers to the form (assemblage of slopes) and pattern of forms expressed by a surficial material on the land surface (Table 4). This three-dimensional shape of the material is equivalent to 'landform' used in a non-genetic sense (e.g., ridges or plain). Surface expression symbols also describe the manner in which unconsolidated surficial materials relate to the underlying substrate (e.g., veneer). Surface expression is indicated by up to three lower case letters, placed immediately following the surficial material designator, and listed in order of decreasing extent.

**Table 4.** Surface expression codes and definitions used in the appended greater Whitehorse surficial geology map unit classifications. Starred items highlight additions or deviations from the BC terrain classification system. Note: the BC slope steepness codes “j”, “a”, “k” and “s” are not used in Yukon.

a	apron*	a wedge-like slope-toe complex of laterally coalescent colluvial fans and blankets; longitudinal slopes are generally less than 15° (26%) from apex to toe with flat or gently convex/concave profiles
b	blanket	a layer of unconsolidated material thick enough (>1 m) to mask minor irregularities of the surface of the underlying material, but still conforms to the general underlying topography; outcrops of the underlying unit are rare
c	cone(s)	a cone or sector of a cone, mostly steeper than 15° (26%); longitudinal profile is smooth and straight, or slightly concave/convex; typically applied to talus cones
d	depression(s)	circular or irregular area of lower elevation (hollow) than the surrounding terrain and delimited by an abrupt break in slope; side slopes within the depression are steeper than the surrounding terrain; depressions are two or more metres in depth
f	fan(s)	sector of a cone with a slope gradient less than 15° (26%) from apex to toe; longitudinal profile is smooth and straight, or slightly concave/convex
h	hummock(s)	steep-sided hillock(s) and hollow(s) with multidirectional slopes dominantly between 15–35° (26–70%) if composed of unconsolidated materials, whereas bedrock slopes may be steeper; local relief >1 m; in plan, an assemblage of non-linear, generally chaotic forms that are rounded or irregular in cross-profile; commonly applied to knob-and-kettle glaciofluvial terrain
l	delta*	landform created at the mouth of a river or stream where it flows into a body of water; typically consists of a gently sloping channeled surface between 0–3° (0–5%) with a moderate to steeply sloping delta front between 16–35° (27–70%)
m	rolling	elongate hillock(s); slopes dominantly between 3–15° (5–26%); local relief >1 m; in plan, an assemblage of parallel or subparallel linear forms with subdued relief (commonly applied to bedrock ridges and fluted or streamlined till plains)
p	plain	a level or very gently sloping, unidirectional (planar) surface with slopes 0–3° (0–5%); relief of local surface irregularities generally <1 m; applied to (glacio)fluvial floodplains, organic deposits, lacustrine deposits and till plains
r	ridge(s)	elongate hillock(s) with slopes dominantly 15–35° (26–70%) if composed of unconsolidated materials; bedrock slopes may be steeper; local relief is >1 m; in plan, an assemblage of parallel or subparallel linear forms; commonly applied to drumlinized till plains, eskers, morainal ridges, crevasse fillings and ridged bedrock
t	terrace(s)	a single or assemblage of step-like forms where each step-like form consists of a scarp face and a horizontal or gently inclined surface above it; applied to fluvial and lacustrine terraces and stepped bedrock topography
u	undulating	gently sloping hillock(s) and hollow(s) with multidirectional slopes generally up to 15° (26%); local relief is >1 m; in plan, an assemblage of non-linear, generally chaotic forms that are rounded or irregular in cross-profile
v	veneer	a layer of unconsolidated materials too thin to mask the minor irregularities of the surface of the underlying material; 10 cm–1 m thick; commonly applied to eolian/loess veneers and colluvial veneers
w	mantle of variable thickness	a layer or discontinuous layer of surficial material of variable thickness (typically 0–3 m) that fills or partly fills depressions in an irregular substrate; generally too thin to mask prominent irregularities in the underlying material
x	thin veneer	very thin layer of unconsolidated material about 2–20 cm in thickness

## Age

Age is only assigned to materials deposited during a specific glaciation (*i.e.*, till, glaciofluvial and glaciolacustrine materials). Within the greater Whitehorse area, these mapped materials were all deposited during the McConnell glaciation (late Wisconsinan, marine isotope stage 2), which is indicated by the “M” following the surface expression.

## Geomorphological processes

Geomorphological processes are natural mechanisms of weathering, erosion and deposition that result in the modification of the surficial materials and landforms at the earth’s surface. With the exception of the deglacial processes, which are assumed to be inactive, all remaining processes are assumed to be active unless the qualifier “I” (inactive) is used. Up to three upper case letters may be used to indicate processes; these are listed in order of decreasing importance and are placed after the surface expression symbol, following a dash (-) symbol (Table 5).

**Table 5.** Geomorphological process and subclass codes and definitions used in the appended greater Whitehorse surficial geology map unit classifications. Starred items highlight additions/deviations from the BC terrain classification system.

<b>Erosional Processes</b>		
-V	gully erosion	running water, mass movement and/or snow avalanching, resulting in the formation of parallel and subparallel, long, narrow ravines
<b>Fluvial and Hydrological Process</b>		
-M	meandering floodplain	a clearly defined channel characterized by a regular and repeated pattern of bends with relatively uniform amplitude and wave length
-U	inundation	terrain seasonally under standing water which results from high watertable <i>Subclass: (b) beaver damming*</i>
<b>Mass Movement Processes</b>		
-F	slow landslide	slow downslope movement of masses of cohesive or non-cohesive surficial material and/or bedrock by creeping, flowing or sliding
-R	rapid landslide	rapid downslope movement by falling, rolling, sliding or flowing of dry, moist or saturated debris derived from surficial material and/or bedrock
-L	undifferentiated landslide*	mass movement of undifferentiated velocity  <i>Subclasses: (b) rockfall; (c) soil creep; (d) debris flow; (e) earthflow; (f) debris fall; (g) rock creep; (k) tension cracks; (m) slump in bedrock; (r) rockslide; (s) debris slide; (u) slump in surficial material; (x) slump-earthflow</i>
<b>Periglacial Processes</b>		
-C	cryoturbation	movement of surficial materials by heaving and/or churning due to frost action (repeated freezing and thawing)
-N	nivation	erosion of bedrock or surficial materials beneath and along the margin of snow patches by freeze-thaw processes (frost shattering and heave), meltwater action and snow creep
-S	solifluction	slow gravitational downslope movement of saturated unfrozen overburden across a frozen or otherwise impermeable substrate
-X	permafrost	processes controlled by the presence of permafrost, and permafrost aggradation or degradation
-Z	general periglacial processes	solifluction, cryoturbation and nivation, possibly occurring in a single polygon
<b>Deglacial Processes</b>		
-E	channeled by glacial meltwater	erosion and channel formation by meltwater alongside, beneath, or in front of a glacier
-H	kettled	depressions in surficial materials resulting from the melting of buried glacier ice
-T	ice-contact*	landforms that developed in contact with glacier ice such as kames








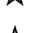









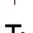
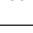
Up to two lower case subclasses may be used following each geomorphological process. Note that subclass codes may have different meanings depending on the associated geomorphological process (e.g., “f” represents debris fall when combined with -L, or thaw flow slides when combined with -X).

## Spatial data

The greater Whitehorse surficial geology map is provided both as a series of ten 1:15 000 scale map sheets in PDF format (Appendix 1, Sheets 1–10), and as digital spatial data in ArcGIS geodatabase format (Appendix 2). The geodatabase contains three primary feature classes: “surficial\_points”, “surficial\_lines” and “surficial\_polygons”. ArcMap project and layer files are also provided with standard symbology that can be imported into ArcGIS Pro if desired. All data are supplied in the NAD 1983 UTM Zone 8N coordinate system.

## Points

The following point features are included in the “surficial\_points” feature class, which is symbolized in the legend by unique values in the TYPE and SUBTYPE fields (Fig. 22)<sup>1</sup>.

TYPE, SUBTYPE	
	drill hole, unclassified
	drill hole, water well
	gravel pit, active or recently active
	gravel pit, historical
	ground observation site, unclassified
	kame, unclassified
	kettle hole, unclassified
	landslide, active layer detachment
	landslide, debris flow
	landslide, retrogressive thaw flow
	landslide, unclassified
	mine, open pit mine
	permafrost mound, unclassified
	sand dunes, cliff top
	spring, unclassified
	stratigraphic section, unclassified
	streamlined landform, ice-flow direction known, drumlin or drumlinoid
	streamlined landform, ice-flow direction known, striae or grooves
	thermokarst collapse, unclassified

**Figure 22.** Standard point symbol legend and feature types included within the appended greater Whitehorse surficial geology map.

<sup>1</sup> Note that custom fonts “gsc3.ttf” and “gsc4.ttf” (included in the digital open file) must be installed on your computer for standardized point symbology to display. To install the fonts, double click them in Windows Explorer/file manager and press “install”, or copy them into your system font folder (usually located at C:\Windows\Fonts).

## Lines

The following line features are included in the “surficial\_lines” feature class. The majority of the features are classified in the legend by unique values in the TYPE and SUBTYPE fields (Fig. 23).

Geological boundaries are classified in a separate layer by unique values in the TYPE, VALIDITY and AGE fields. All line features which form polygon contacts are tagged where the BOUNDARY field = “Y”.

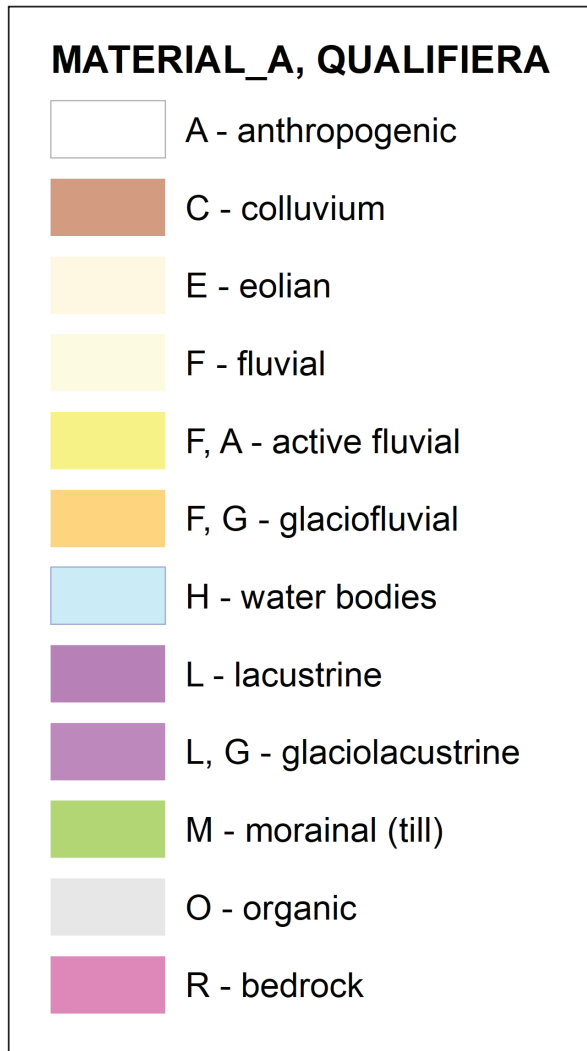
<b>surficial_lines (geological boundaries)</b>	
<b>TYPE, VALIDITY</b>	
———	geological boundary, defined
----	geological boundary, approximate
.....	geological boundary, assumed
<b>surficial_lines (other)</b>	
<b>TYPE, SUBTYPE</b>	
———	berm or dyke, unclassified
.....	cross section profile, ERT transect
.....	cross section profile, unclassified
———	escarpment, gravel pit
	escarpment, unclassified
>>>>>	esker, flow direction known, unclassified
++ +	glacial lake shoreline, unclassified
+→	gully, unclassified
——→	ice-flow direction, unclassified
——→	landslide direction of movement, unclassified
	landslide headwall scarp, unclassified
———	landslide, unclassified
-----	limit of mapping, unclassified
--- --	lineament, tension joint
——→	meltwater channel, major, flow direction, unclassified
▲▲	meltwater channel, major, unclassified
——→	meltwater channel, minor, flow direction known, unclassified
———	meltwater channel, minor, flow direction unknown, unclassified
●●	moraine ridge, unclassified
~~~~~	sand dunes, unclassified
++ +	shoreline, unclassified
——→	streamlined landform, ice-flow direction known, undifferentiated lineations and flutings
——→	water track, unclassified

**Figure 23.** Standard line symbol legend and feature types included within the appended greater Whitehorse surficial geology map.

## Polygons

Features in the “surficial\_polygons” feature class are classified by unique values in the MATERIAL\_A and QUALIFIERA fields (Fig. 24). Note that the map is therefore only coloured by the first terrain unit (MATERIAL\_A).

Polygons should be labelled with the “LABEL\_FNL” field (for complete labels), or the “LABEL\_SIMP” field (for simplified labels with no textures or ages).



**Figure 24.** Standard polygon legend classified by primary surficial material type (MATERIAL\_A and QUALIFIERA fields) in the appended greater Whitehorse surficial geology map.



## Geohazards

The primary geohazards present within the study area include landslides, radon gas, seismicity, permafrost and flooding. Each type of geohazard is addressed in more detail in subsequent sections.

### Landslides

Landslides occur in a variety of settings within the greater Whitehorse area. In valley bottoms, landslides exhibit a variety of styles of movement (e.g., debris and earth flows, slides, falls and slumps) and commonly occur along escarpments (e.g., Whitehorse escarpment slides in 2022) and active cutbanks of the Takhini and Yukon rivers. Gullying is also common, particularly within glaciolacustrine sediments.

Active-layer detachments are found on north and east-facing, subalpine colluvial/till slopes, which are underlain by permafrost. These are shallow, relatively small failures (typically <2 m deep, <100 m long and <20 m wide) that are often triggered by forest fires (e.g., Haeckel Hill; Huscroft et al., 2004).

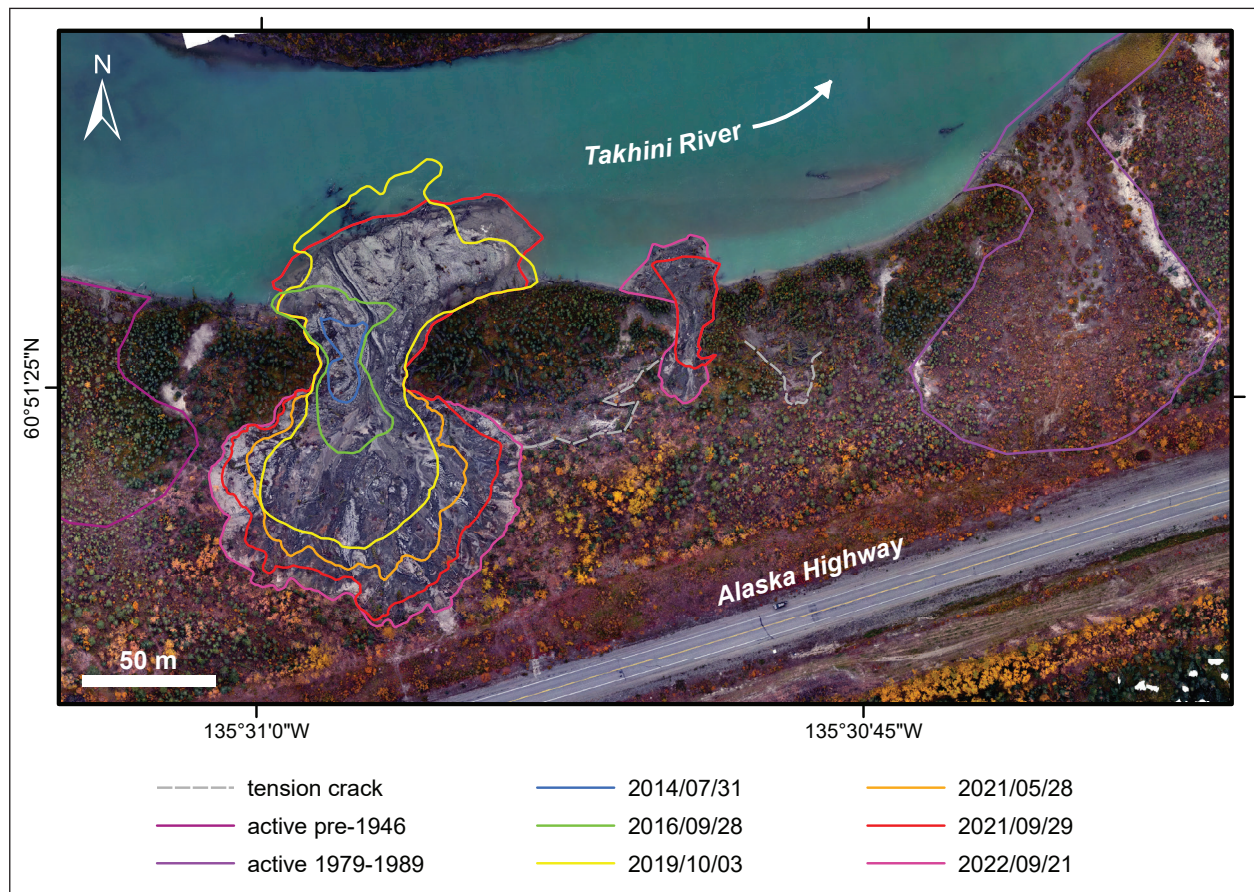
Retrogressive thaw flows (commonly referred to as slumps) are another permafrost-related landslide that typically occurs within ice-rich glaciolacustrine materials along riverbanks, although they locally occur in mid-slope topographic positions within till (e.g., the 2010 failure in the headwaters of Little Takhini Creek; Fig. 25). The Takhini River retrogressive thaw flow (Figs. 26 and 27), located in the Ibex Valley at approximately KM 1456.5 of the Alaska Highway, is another recent and dramatic example of this type of landslide (documented in detail in Roy et al., 2021 and Calmels et al., 2021).



**Figure 25.** This landslide occurred in May 2010 on the eastern flanks of Haeckel Hill. The slide adversely impacted water quality in Little Takhini Creek. Approximately 10 m of till was exposed in the headscarp. While permafrost was not confirmed in the headscarp, the morphology and site characteristics suggest it is a retrogressive thaw flow. September 2010 photo by Cameron Eckert.



**Figure 26.** Oblique UAV photos of Takhini River retrogressive thaw flow, September 21, 2021 (**a**) and September 21, 2022 (**b**); Peter von Gaza photos. View is to the southwest, looking upstream; note vehicle on highway for scale (**a**). The thaw flow initiated in 2014 as a small failure similar in size to the one in the lower left corner of the upper photo. This smaller slide initiated as an active layer detachment in September 2021, and transitioned into a retrogressive thaw flow the following year.

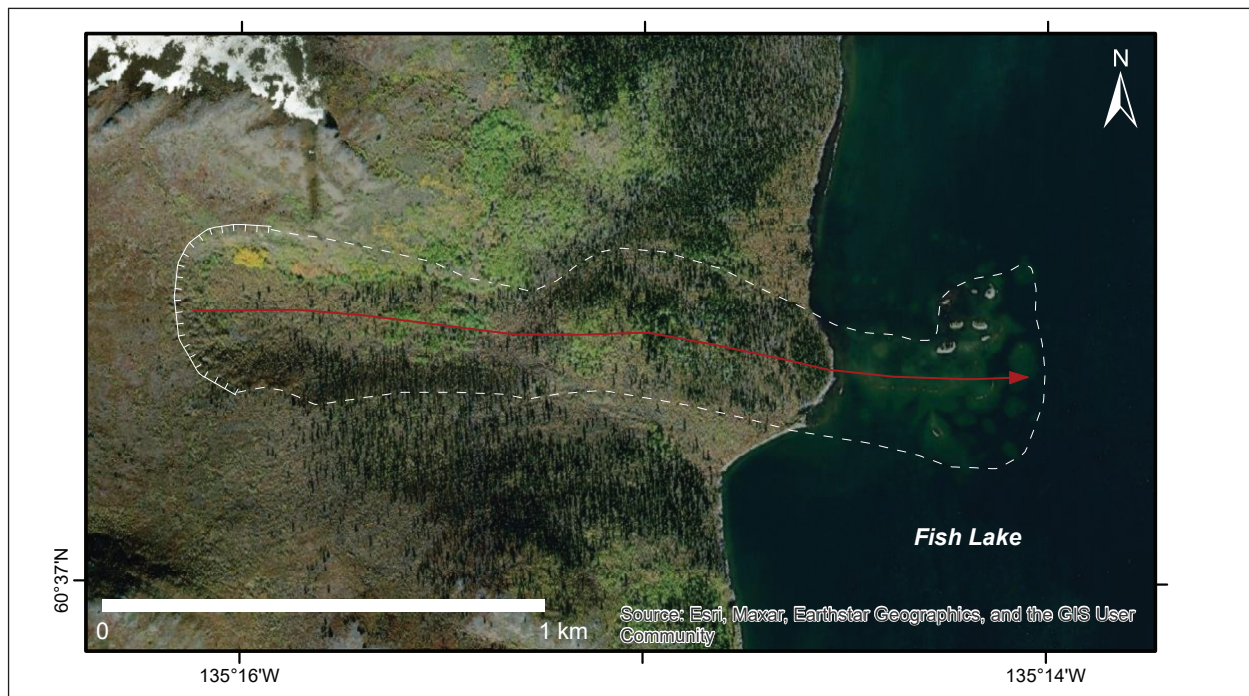


**Figure 27.** Evolution of Takhini River retrogressive thaw flow from 2014 to 2022. The headwall has retreated toward the highway at an average rate of up to 10.8 m/year since 2014. On September 29, 2022 (date of background UAV orthophoto), the headwall was within 31 m of the Alaska Highway embankment. The smaller slide in the center of the image developed in September 2021 and retreated 14 m during the summer of 2022. Two adjacent large thaw flows to the west and east were active prior to 1946 and in the 1980s, and have since stabilized.

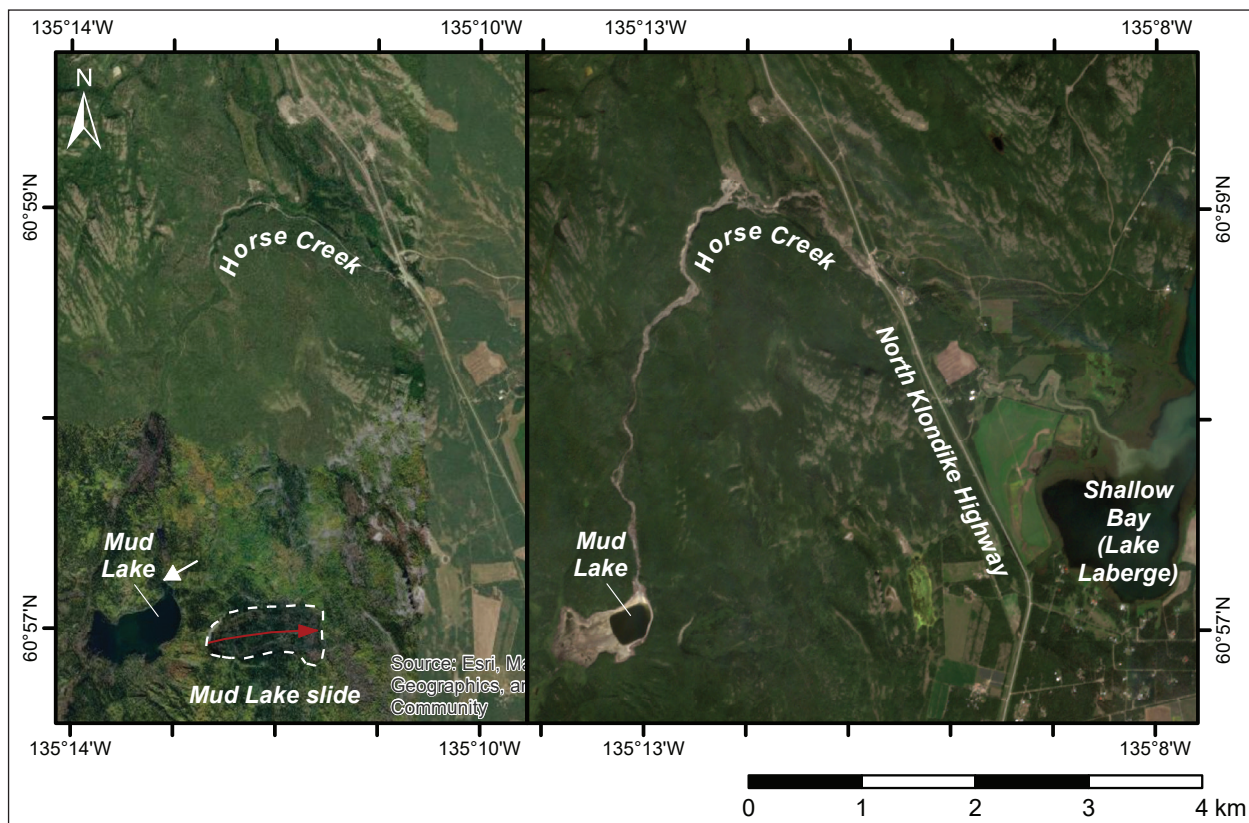
The two largest known landslides in the study area occurred at Fish Lake (Fig. 28) and Mud Lake (Fig. 29), with two and one kilometre runout distances respectively. Based on the muted morphology of the scars and deposits, both of these events are assumed to be prehistoric and likely occurred thousands of years ago following the last deglaciation. Due to the extensive runout distances, and the fact that bedrock occurs near surface near the source zones, these events are interpreted as rockslides or rock avalanches.

Another geohazard that has been recently documented is outburst flooding and washouts caused by catastrophic beaver dam failures. On July 4, 2022, a beaver dam failure occurred at Mud Lake, causing a torrent that scoured and widened parts of the Horse Creek floodplain (Fig. 29). Cutbanks up to 10 m high were carved in some locations, and the level of Mud Lake dropped an estimated 1.3 m (D. Holcombe, pers. comm., 2022). Approximately five kilometres downstream from Mud Lake, the flood waters washed over the North Klondike Highway, causing lane closures, and undercutting parts of the road embankment, culvert and guardrails<sup>2</sup>. A large sediment plume was also deposited into Lake Laberge at the mouth of Horse Creek, about 8 km downstream from Mud Lake.

<sup>2</sup> Newspaper source: <https://www.cbc.ca/news/canada/north/klondike-highway-yukon-flood-partial-closure-1.6510441>



**Figure 28.** A 2 km long ancient landslide on the west side of Fish Lake. Small islands are formed from the landslide debris. September 20, 2018, WorldView2 satellite image background.



**Figure 29.** Satellite imagery comparison of Mud Lake area before (left; September 20, 2018 WorldView2) and after (right; August 19, 2022 Sentinel-2) beaver dam outburst flood on July 4, 2022. White arrow points to location of burst beaver dam. Note partially drained Mud Lake and scoured Horse Creek floodplain after flood. Location of ancient Mud Lake landslide is also marked.

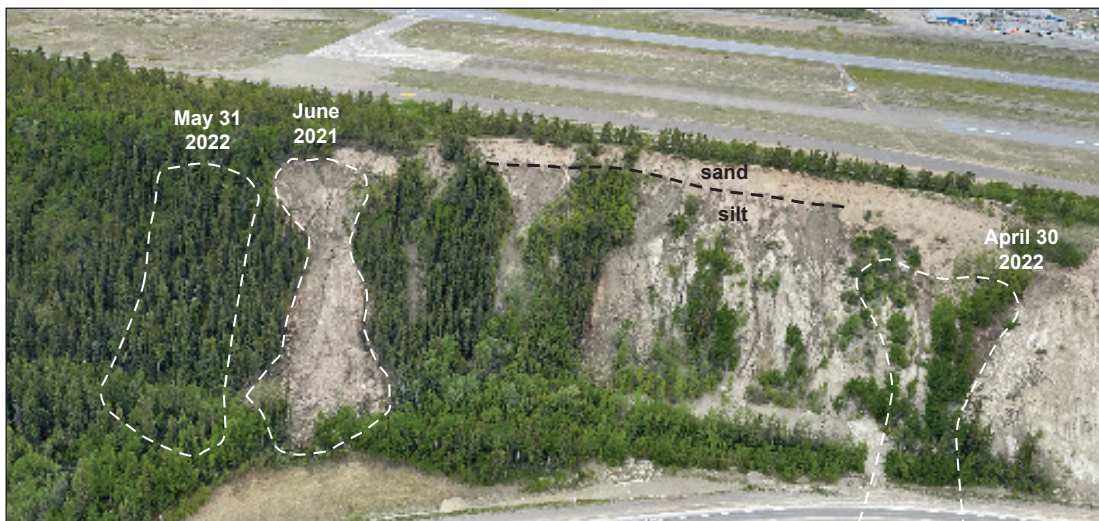
A similar beaver dam outburst washout occurred on the same day at Contact Creek, at KM 898 of the Alaska Highway (about 80 km south of Watson Lake). This event closed the highway for three days and caused major traffic disruptions and shortages of retail supplies in Whitehorse. The cost to repair the 75 m section of washed out highway was \$2.6 million<sup>3</sup>, which highlights the destructive potential of these events.

## 2022 Whitehorse escarpment slides

During the spring of 2022, an unprecedented number of landslides occurred along the Whitehorse escarpment (the steep bluff approximately 60 m high that separates the airport and runway from downtown Whitehorse). The slides significantly affected local transportation infrastructure, recreation, and housing. Robert Service Way was closed for nearly seven weeks causing major traffic disruptions, and mitigation measures costing approximately half a million dollars were implemented. Evacuation orders were issued for three homes, a playground was removed at the south end of town, and a variety of recreational trails were closed for several weeks.

The first of these slides occurred on Robert Service Way on April 30, followed by four others about a month later near Drury, Wood, and Jeckell streets, and again above Robert Service Way. While landslides are a common occurrence along the Whitehorse escarpment, to date, there have never been so many of this magnitude documented in the same year, or so early in the season. Prior to 2022, only a handful of other slides of similar size have been documented in historical times, including the following events:

- a large earth flow on Robert Service Way in early June 2021 (Fig. 30);
- a large slide in July 2000 below Takhini East subdivision and above Marwell industrial area (Fig. 31; EBA, 2002);
- two slides in June and July 1953 which damaged roads and buildings at the heads of Hoge St. and Steele St. (Fig. 32; Legget and Johnston, 1959); and
- two major events in July 1949 (Legget and Johnston, 1959).



**Figure 30.** The early June 2021 earthflow initiated in a pre-existing gully bowl and ran out within 35 m of Robert Service Way (June 11, 2021 photo). Approximate locations of 2022 slides are also outlined to highlight pre-failure slope conditions. Approximate boundary between sand and silt marked by black dashed line.

<sup>3</sup> Newspaper source: <https://www.yukon-news.com/news/contract-awarded-for-repair-of-alaska-highway-washout/>



**Figure 31.** The headscarp area of the July 2000 Takhini East slide continues to actively retreat (May 5, 2022 photo).



**Figure 32.** June 1953 slide near Hoge Street (1957 photo in Legget and Johnston, 1959).

## ***Historical background***

Some of the earliest infrastructure to be impacted by landslides in the Whitehorse area was the White Pass and Yukon Route railway circa 1900 (Brideau et al., 2011). Airport development began on the bench above downtown beginning in 1920, with further expansion in the 1940s. The airport terrace was heavily deforested at the time of development and construction, which has been cited as an important factor contributing to ongoing slope instability (EBA, 2002). An airport access road extending up the face of the escarpment from the west end of Main Street was built in 1937, but was abandoned in 1953 due to persistent slides and maintenance issues. The bottom of this road now serves as a diversion berm for mudflows from above.

A number of engineering studies that focussed on the escarpment instability were completed as far back as the 1950s. This work resulted in the establishment of a 'set forward line' in the early 1970s regulating city development. In 1974, 130 downtown lots behind this line were identified for expropriation under a federal funding program. Of these, 80 properties were bought out at fair market value. It is worth noting that the 1970s expropriation effort has probably saved several lives and significant damage costs. At least four of the expropriated lots would have been impacted by the 2022 Wood Street and Drury Steet slides. Furthermore, three buildings present in 1968 air photos would also have been impacted by the 2022 Jeckell Street slide.

In 2002, EBA established geohazard rating zones (high, medium and low) for the escarpment area, to better guide city development. Currently, there is no development permitted in the high hazard zone. In the medium hazard zone, building development is generally not recommended, but may occur if deemed appropriate after a site-specific slope stability assessment, and any necessary mitigation measures are implemented (e.g., deflection berms and reinforced concrete basement walls). The low hazard zone is defined as having a 10% or less chance of a damaging event occurring in 50 years.

In 2012, the city also established the Downtown Whitehorse Escarpment Control Zone, which prohibits human habitation within its bounds.

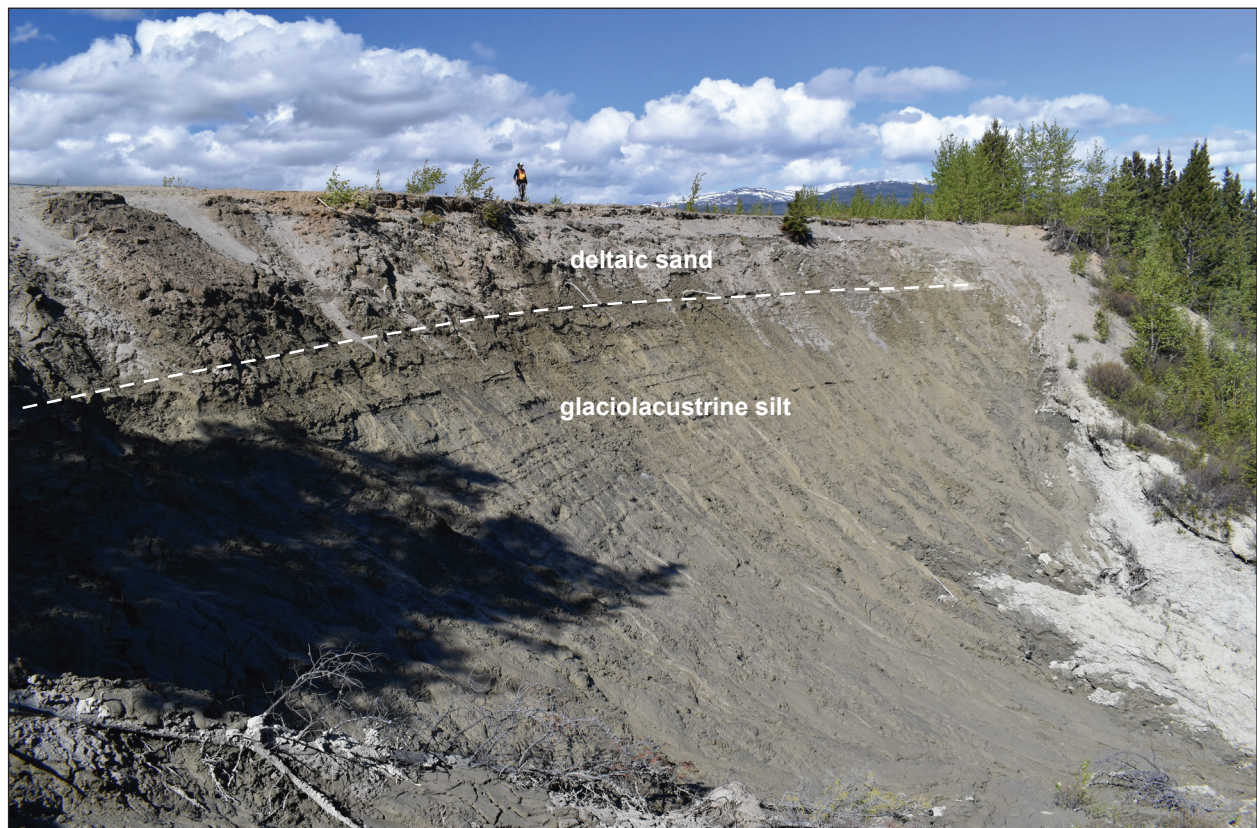
## ***Geological background***

The generalized stratigraphy of the Whitehorse escarpment consists of a blanket of deltaic sand at the top of the escarpment, overlying glaciolacustrine sediments that are up to at least 100 m thick (Fig. 33). The deltaic sand unit consists of clean, medium to coarse-grained sand, with minor amounts of gravel. This unit has an average thickness of 3–5 m (EBA, 2002), but locally, may be as much as 9 m thick (Legget and Johnston, 1959). On average, the glaciolacustrine sediments consist of about 3/4 silt with the remainder split between fine sand and clay (EBA, 2002), thus the informally used term "clay cliffs" is not technically correct. Although a range of textural and structural variations occur (Brideau et al., 2011), the glaciolacustrine sediments are commonly finely laminated or horizontally layered, very cohesive and compact, and can maintain very steep slopes when dry. Finer and coarser grained beds within the glaciolacustrine sediment will also affect local drainage patterns by inhibiting, or transmitting groundwater flow, respectively.

Legget and Johnson (1959) generated a contour map of the top surface of the glaciolacustrine unit (i.e., the contact between the silt and sand units), based on analysis of more than 500 boreholes. This map illustrates that the surface is not flat, which is likely a result of fluvial modification by scouring and carving of paleochannels across the former delta surface. Future detailed characterization of these channels would be beneficial, as they may be directing groundwater flow towards focused areas on the face of the escarpment.

Colluvium is also a significant surficial geological unit on the escarpment. It forms through the remobilization of sand and silt under the force of gravity, gradually accumulating on moderately steep slopes and in gullies. Colluvium on the escarpment slowly builds up through the action of seepage or weeping processes, as well as processes such as soil creep, raveling, shallow

sloughing, groundwater sapping (Eyles et al., 1985), and small-scale landslide processes that only run part way down the slope. Colluvium commonly forms a veneer or blanket of material up to a few metres thick on the surface slope of the escarpment. It generally has a platy structure with bedding parallel to the slope, and may incorporate fragments of organic material, or buried soil horizons. This colluvium is looser, more porous, and inherently weaker than the underlying, very compact glaciolacustrine sediment, which often acts as a sliding plane or failure surface.



**Figure 33.** Exposure of deltaic sand overlying horizontally bedded glaciolacustrine silt on the upper slope of the Whitehorse escarpment above Main Street (18PL004). Note person at the top of the escarpment for scale.

### ***Landslide mechanisms***

When colluvium becomes saturated on steep slopes, it can become highly susceptible to failure and landslide activity. This typically occurs during periods of excessive rainfall, snowmelt, and/or high groundwater levels. Along the escarpment, the contact between the deltaic sand and the glaciolacustrine silt strongly influences the delivery of groundwater to the steep slope faces. Because sand is so porous, it allows rainfall and snowmelt to percolate quickly down to the less permeable silt below. The groundwater is then forced to seep laterally along this interface, until it is expelled out onto the face of the escarpment.

Antecedent precipitation is another important factor that influences slope instability. Extreme rainfall is a known trigger for slides on the escarpment, particularly after longer periods of wetter weather. Two consecutive winters of extreme snowfall also occurred leading up to the spring of 2022. At the Whitehorse airport, cumulative precipitation was 161% of the climate normal for the period between October 2021 and April 2022 (Yukon Water Resources Branch, 2022). In both 2021 and 2022, the snow survey bulletins reported the April 1 snowpack and overall winter snowfall as 1.5 to 2 times higher than normal levels.



Snowfall has direct links on local groundwater levels, as snowmelt in the early spring typically causes a very rapid rise in groundwater levels, abruptly flooding the subsurface recharge zone. This generates a layer of ground at depth that suddenly becomes saturated during freshet, and promotes conditions that are more unstable. Not only was the April 2022 freshet recharge likely far above normal, unstable conditions were compounded by elevated groundwater levels that pre-existed in response to the previous year's extreme snowfall. This pulse of above-average snowmelt infiltrating into the ground in April 2022 ultimately resulted in substantially more saturated ground in the subsurface than is considered normal.

Landslides are traditionally classified according to the style of movement, and the grain size of the failed material (e.g., Varnes, 1978; Hungr et al., 2014). In the case of the Whitehorse escarpment, the material involved in the slides was generally limited to sand, silt and clay, which is referred to as earth (or mud when heavily saturated), as opposed to coarser grained sediment incorporating gravel and larger clasts, which would be referred to as debris. The sediment may move down the slope in one, or a combination of movement styles, which primarily consist of slides and flows along the Whitehorse escarpment. In slides, slabs of sediment move downslope along a roughly planar surface. Flows involve the mobilization of heavily saturated sediment that is often confined to a gully, and then fans out at the base of the slope.

Gullies form when water and saturated sediment travel down pre-existing channels on the escarpment face in repeated events. This process is especially active during spring snowmelt season. Mudflow gullies often have a bowl-shaped source zone rimmed by steep walls or headscarps. Colluvium often accumulates in the source zone bowls where sediment becomes saturated from snowmelt, seepage, and sapping (e.g., Eyles et al., 1985) along the sand/silt interface. The saturated material generally seeps down open slopes and gullies in relatively small magnitude events, and locally gets flushed down the gullies in larger mudflows. Low-angle colluvial fans composed of this saturated material often extend well beyond the base of the escarpment.

In order to contain mudflows and protect homes and municipal infrastructure, several mitigation methods have been recommended and/or implemented in Whitehorse over recent years (EBA, 2002, 2012). These include construction of berms, interception ditches, and settling ponds; restricting construction of basements and windows near the ground; reinforcing foundations; and revegetating/reforesting the rim of the airport plateau.

The bowls at the tops of the gullies also trap windblown snow, which forms snowbanks that persist into the late spring, further exacerbating mudflow activity as the snow melts. The removal of tree cover from the airport surface has ultimately promoted greater snow accumulation in these bowls. Furthermore, overhanging snow cornices often develop, which present a significant avalanche hazard during winter; in fact, one avalanche fatality occurred on the escarpment above Black Street in the 1970s.

#### *April 30, 2022 Robert Service Way slide*

This was the first major landslide to occur on the escarpment in 2022 (Fig. 34). The slide initiated from a partially vegetated 45 m-wide source zone located just below the sand/silt interface (see Fig. 30). It dropped about 55 vertical metres, rapidly flowing across Robert Service Way and the Millennium Trail, and onto the Yukon River ice below. The mudflow was extremely mobile due to a very high water content, running out a total of 160 m (about 70 m from the base of the escarpment).

Despite the relatively thin debris, which averaged about half a metre thick across the road and up to 1.5 m thick on the river ice, the force of this slide was enough to transport mature trees, bend railroad tracks across the road, and rip up guardrails. The total volume of debris was approximately equivalent to one Olympic-sized swimming pool (~2500 m<sup>3</sup>).



**Figure 34.** Slide debris extending across Robert Service Way and Millenium Trail on April 30, 2022.

An eyewitness video (Danielle Bonneau Facebook video posted by CBC Yukon: <https://fb.watch/j64Ci5vud2/>) shows that the event occurred in at least two phases. Reconnaissance investigations suggest that a slab of vegetated colluvium initially slid down a planar slope on the north half of the source zone. This would have eroded material from the foot of the slope, and likely debutressed saturated colluvium that had accumulated in a gully immediately to the south, triggering the second phase mudflow immediately thereafter.

Because this event occurred so early in the thaw season, it is likely that some seasonal frost still existed on, or just below, the surface of the slope. Frozen ground is generally impermeable as ice fills the soil pores, so this may have resulted in a backup of pooled water in the subsurface during percolation of snowmelt. Sudden rupture of the frozen layer may have then released the large volume of pooled water, facilitating the extremely mobile event.

One eyewitness reported a “garden hose” volume of water spurting out of the initiation zone a few days prior to the failure, confirming that high pore water pressures had indeed been building up. Post-failure photos show that seepage continued to occur within the initiation zone, as well as higher up at the sand/silt interface on the steeper bluff to the north.

Robert Service Way was reopened for public use about seven weeks after the slide, following the construction of a 130 m-long sheet pile wall and earth berm; these were built to mitigate the impact of potential further slides in adjacent gullies.

### May 25, 2022 Drury Street slide

The Drury Street landslide was a large earth slide that occurred around 4 pm on May 25th, nearly one month after the first Robert Service Way slide. The pre-failure source slope was sparsely vegetated with grass and shrubs, and exhibited evidence of seepage and active colluviation at least one year prior (Fig. 35). A slab of colluvium approximately 70 m wide and 2–4 m thick detached and slid downslope, flattened a patch of mature forest, and ran out a total of about 95 m. The debris was relatively dry, measured up to about 3.5 m thick, and extended up to 40 m from the base of the cliff to within 30 m of a home (Fig. 36). Field observations on the following day noted very saturated ground adjacent to the initiation zone (Fig. 37), and no evidence of seasonal frost was observed above, or on, the failure surface.

Analysis of lidar imagery shows that the Drury Street slide initiated just above the inflection point between the shallower (24°) upper slope, and the steeper (39°) mid to lower slope (Fig. 38). This pattern was also observed at all the subsequent escarpment slides that occurred in 2022.



**Figure 35.** Drury Street slide area (outlined) prior to the May 25th, 2022 event (June 2021 photo). Arrows highlight recent colluvial activity in the initiation zone area.



**Figure 36.** View looking down Drury Street slide from the headscarp (May 27, 2022 photo).



**Figure 37.** Tension crack in saturated ground adjacent to Drury Street slide source zone (May 26, 2022; Jeff Bond photo).



**Figure 38.** Drury Street slide source zone (May 26, 2022; Jeff Bond photo).

#### *May 27, 2022 Wood Street slide*

The Wood Street landslide (Fig. 39) was another large earth slide that occurred on a maturely forested colluvial slope, pushing over mature trees across a recreational footpath. Measuring approximately 40 m wide and 70 m long, the Wood Street slide had a much shorter runout than the other 2022 escarpment slides, only travelling about 15 m past the base of the escarpment. This is likely due to drier source materials as the upper slope was flanked by two large gully bowls that capture most of the nearby slope drainage. The slide initiated just above the inflection point between a 30° upper slope, and a 43° lower slope. A smaller slide also occurred on the northern flank of this slide nine days prior, on May 18<sup>th</sup> (Fig. 40), suggesting that smaller events may sometimes serve as an early warning of larger subsequent events.

#### *May 28, 2022 Jeckell Street slide*

The Jeckell Street slide occurred at 10:36 am on May 28, 2022. The slide was caught on video (<https://fb.watch/j64OsvbYlj/>) using a trail camera installed by Yukon Geological Survey, less than 24 hours before the slide occurred. The camera was positioned above a prominent tension crack approximately one metre deep that faced downslope. The earth slide moved translationally along a planar failure surface (with several trees remaining upright) and ran out 50 m from the base of the escarpment (Figs. 41 and 42). The slide initiated just above the inflection point between a 22° upper slope, and a 40° mid-lower slope; it measured approximately 45 m wide, 47 m high, and 105 m long from head to toe. The debris ran onto the corner of Jeckell Street and 6<sup>th</sup> Avenue, reaching within 15 m of a home, and buried part of a playground, which had been previously fenced off by the city.



**Figure 39.** The May 27, 2022 Wood Street slide did not travel far past the base of the escarpment, but nonetheless, pushed mature trees across a recreational path.



**Figure 40.** A small precursor slide occurred on May 18, 2022 on the north flank of the May 27, 2022 Wood Street slide.



**Figure 41.** View looking down Jeckell Street slide from the headscarp (May 28, 2022 photo).



**Figure 42.** View of Jeckell Street slide debris, which engulfed a playground swing set. Initiation zone and failure plane are visible in the background.

### *May 31, 2022 Robert Service Way slide #2*

On May 31, 2022, a second slide occurred along Robert Service Way, about 250 m south of the first event on April 30 (Fig. 43). The large earth slide measured approximately 105 m long, 40 m wide, and 50 m high; the run out was 35 m past the base of the escarpment, reaching to within 45 m of Robert Service Way. The slide initiated on a colluvial slope just above the inflection point between the 26° upper slope, and the 36° mid-lower slope. The sliding depth in the initiation zone ranged between approximately 2 and 4 m, and debris thicknesses up to 3.5 m were measured using lidar imagery (collected June 19, 2022).



**Figure 43.** Initiation zone and failure plane of May 31, 2022 earth slide off Robert Service Way (October 10, 2022 photo).

### ***Implications***

The 2022 Whitehorse escarpment slide activity demonstrates that detailed landslide hazard analysis needs to be a crucial component of all infrastructure planning, construction, and maintenance projects that are located, or proposed, anywhere near colluvial slopes on moderately steep terrain. The Wood Street and second Robert Service slides serve as important reminders that what may appear to be a stable slope (i.e., maturely forested slope with no recent evidence or history of landslides) may still be susceptible to instability under certain conditions. Professional interpretation of good quality imagery and baseline data such as lidar and surficial geology maps are critical in identifying potential areas of instability. During periods of known or suspected instability, ground survey inspections and monitoring programs are essential for quickly identifying small-scale instability features such as tension cracks, split or tilted trees (e.g., Fig. 44), saturated ground, and minor slides that may provide early warning of subsequent larger events. Closely monitoring groundwater levels near sites of potential instability would also be valuable during such periods.





**Figure 44.** Indicators of active slope instability include fresh tension cracks, often spanned by outstretched roots (left) and split trees (right). May 2022 photo taken just south of slide in the Takhini East subdivision.

### ***Future research opportunities***

The following are some recommendations to improve future understanding of the slope instability along the escarpment:

1. Continue ground-based monitoring efforts, such as survey monuments, extensometers, and trail cameras, particularly during periods of known or suspected instability, as well as repeat lidar surveys for change detection at regular intervals (minimum annually).
2. Investigate the morphology of the sand/silt interface surface and the distribution of paleochannels using modern geophysical techniques, and a complete compilation of airport geotechnical data within a 3D subsurface modelling platform to understand groundwater movement.
3. Establish a deep groundwater-monitoring program to better understand the influence of groundwater levels on future slides.
4. Characterize the potential effects of seismic events on escarpment slope stability.
5. Consider reforestation and snow management options on the airport bench, such as snow fencing and snow removal practices.
6. Encourage citizen science and establish a method for members of the public to report potential signs of instability (such as tension cracks, split trees, and recent slides), for example, by using the City of Whitehorse's trouble line.

## Radon

Radon is an odourless, colourless, radioactive gas produced by the radioactive decay of naturally occurring uranium found in soil and bedrock. Long-term radon exposure is cited by Health Canada as the leading cause of lung cancer in non-smokers, while the annual number of deaths in Canada from radon-induced lung cancer is more than 1.5 times that from car accidents (<https://takeactiononradon.ca/learn/health-effects/>). Radon gas dilutes to harmless levels in outdoor air, but can concentrate in buildings through inadequately sealed foundations. It is very important to test indoor radon levels in all homes, as they can vary widely based on construction styles, heating and ventilation systems, and local ground conditions.

Figure 45 (see page 46) shows the range of indoor radon concentrations measured in various subdivisions in the greater Whitehorse area. A significant proportion of the homes tested in most of the subdivisions had radon levels higher than Health Canada's recommended limit and required some form of mitigation. In most cases, simple and relatively inexpensive home repair techniques and ventilation improvements can reduce indoor radon levels very effectively ([www.takeactiononradon.ca](http://www.takeactiononradon.ca)).

As part of this study, YGS supported intensive radon surveys conducted by Kishchuk and Kishchuck et al. (2021) who examined a number of geological controls on soil radon at 30 sites around Whitehorse (Fig. 46). He evaluated several parameters, including underlying bedrock lithology, depth to bedrock, surficial material type, grain size distribution, sorting, sediment maturity, soil moisture, matrix, and clast geochemistry. Among his sites, higher soil radon concentrations were measured in till than in glaciofluvial gravel and eolian sand sites, whereas low radon concentrations were measured in fine-grained glaciolacustrine sediments. He also found that less mature or less modified sediments such as till yielded higher radon concentrations than more reworked/weathered sediments such as fluvial and eolian materials. No significant correlation between radon concentration and bedrock lithology or depth to bedrock was found at his sites, suggesting that bedrock is not the sole source of radon in the ground. Kishchuk's results also suggest that the uranium content of near-surface sediment (at 60 cm depth) is not a significant source of radon. Some seasonal variability in soil radon was also observed in three long-term control sites.



**Figure 46.** Radon soil gas control site in till substrate near Squatter's Row subdivision (19PL051).

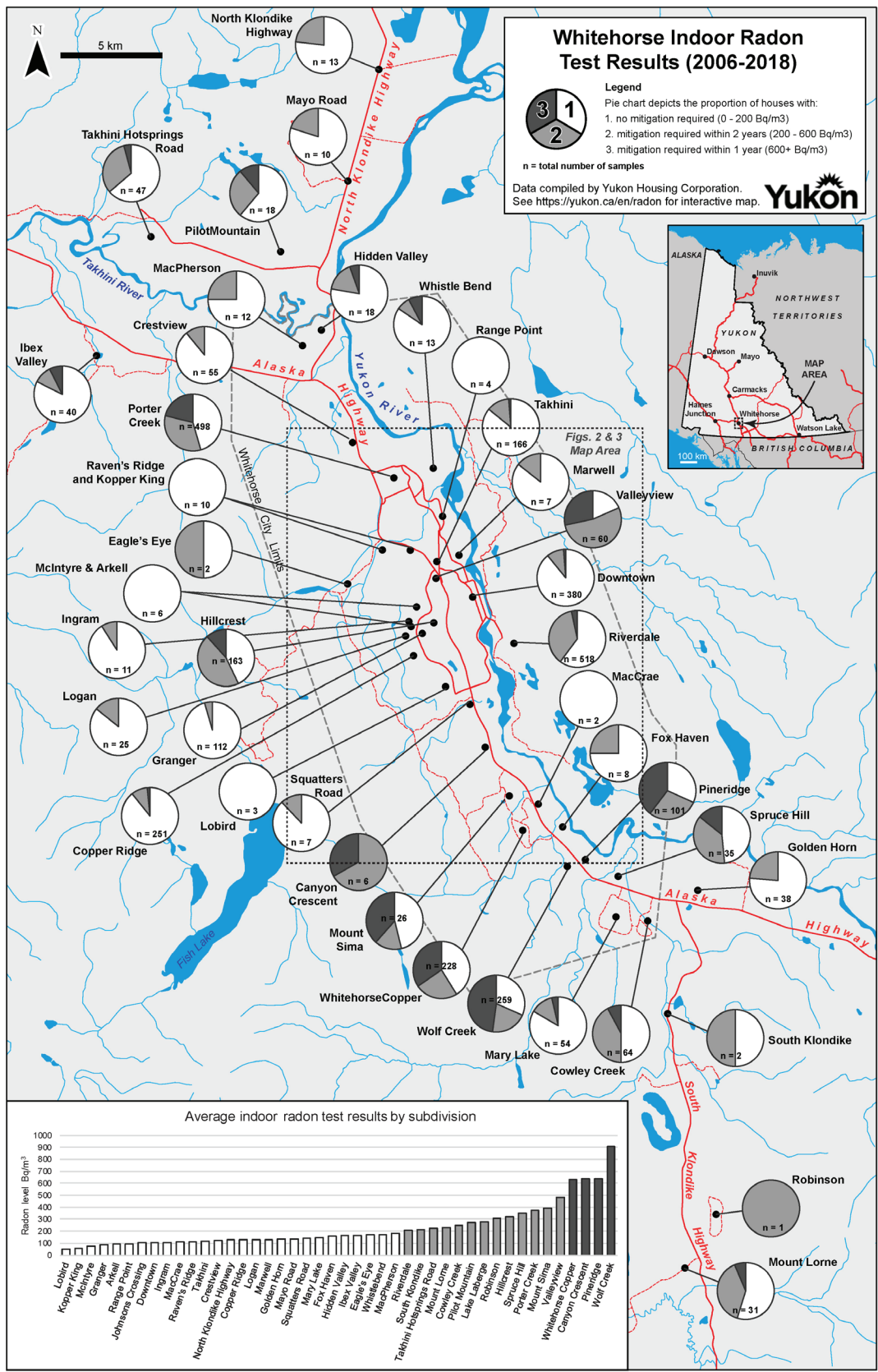


Figure 45. Indoor radon testing results for Whitehorse area (from Kishchuck et al., 2021).

## Seismicity

The study area is located within the moderate seismic hazard zone (Natural Resources Canada, 2015), which has a 5 to 15 per cent chance that significant damage will occur to one or two storey buildings every 50 years. Seismic shaking experienced in the area is most commonly the result of earthquakes that occur more than 100 km away along several major fault systems in southwestern Yukon and neighbouring Alaska, such as the Denali and Duke River faults.

Only three earthquake epicentres occur in the 1897–2021 earthquake record (Natural Resources Canada, 2022) within the map area itself, and they were all very small (magnitude (M) 1.2–2.6). Nine earthquakes between M4 and M5 have been recorded within 100 km of the study area. There have been 115 earthquakes greater than, or equal to, M4 recorded within 200 km of the study area, only 3 of which were greater than M6 (to a maximum of M6.5).

Two of these were the M6.2 and M6.3 earthquakes that occurred in the Haines Pass area on the morning of May 1, 2017, approximately 130 km southwest of downtown Whitehorse. These events caused strong ground shaking, power outages, school closures, minor building damages (Fig. 47), and small landslides (Fig. 48) in the Whitehorse area. (See multiple videos showing shaking and damages here: <https://www.cbc.ca/news/canada/north/earthquake-yukon-alaska-1.4093105>.)



**Figure 47.** Repairing cracks on the exterior of a downtown Whitehorse building, following the May 1, 2017 earthquake (May 9, 2017 photo).



**Figure 48.** Landslide on the Whitehorse escarpment during the May 1, 2017 earthquake (Angie Dickson photo).

Ground shaking intensity felt at a particular location varies depending on proximity to the epicentre, local ground conditions, building type, and topography. The intensity generally increases as you move closer to the epicentre, and is amplified in softer and thicker sediments, or on raised topographic features such as hills, ridges, and cliff tops. The seismic hazard is greatest in areas underlain by thick deposits of soft clay, particularly where they are capped by peat and organic soils; it is lowest where bedrock is at, or near the surface. However, the amount of amplification due to soil conditions does diminish as the strength of ground shaking increases (Monahan et al., 2000).

Strong earthquakes have the potential to trigger landslides, damage infrastructure and buildings, and can cause liquefaction of saturated sandy sediments such as deltaic or fluvial deposits, beach sands, or poorly compacted artificial fills. The likelihood of earthquake-induced landslides is generally greater during larger events, but diminishes rapidly with increasing distance from the epicentre. For example, past studies suggest that a M5 earthquake may trigger landslides up to 15 km away, whereas a magnitude M6 event could trigger them up to 80 km away, and earthquakes smaller than M4 are unlikely to trigger landslides at all (Keefer, 1984 and 2002).

## Permafrost

Permafrost is ground that remains frozen for at least two years. It is overlain by the active layer, which thaws and refreezes annually. The greater Whitehorse area is located within the sporadic discontinuous permafrost zone (Heginbottom, 1995). Permafrost in the study area is largely found in isolated patches where site-specific environmental conditions have allowed permafrost to be preserved. Factors such as surface organic thickness, slope orientation, vegetation cover, local climate, and surficial material texture strongly influence where permafrost occurs, and how much ground ice it contains.

Roy et al. (2021) characterized permafrost conditions in the greater Whitehorse area in detail and conducted field investigations at seven case study sites representing the primary environments where permafrost occurs. The four primary geological settings they describe include low-lying, fine-grained or organic-rich terrain (e.g., within abandoned meltwater channels); fine-grained glaciolacustrine sediments; north-facing slopes underlain by till; and subalpine peat plateaus. The case study sites are located in the vicinities of Cowley Creek, Hamilton Boulevard, Hidden Valley, Ibex Valley, the Old Alaska Highway, and Fish Lake. Roy et al. (2021) found that active layer thicknesses ranged from 0.5 m to greater than 4 m, and the base of permafrost ranged from 2–30 m depth. Among the case study sites, the thickest, most extensive, and most ice-rich permafrost occurred within glaciolacustrine sediments in the Ibex Valley area. Ground temperature monitoring indicates that permafrost throughout the greater Whitehorse area is 'warm' (i.e.,  $> -1^{\circ}\text{C}$ ), and therefore very vulnerable to thaw by disturbance or environmental change.

Roy et al. (2021) also developed a thaw sensitivity model (<https://yukonu.maps.arcgis.com/apps/MapJournal/index.html?appid=e8c7f5a106aa4567bdf53ee7feed3af4>) for the greater Whitehorse area. The model classifies the relative likelihood of developing ground surface disturbance such as subsidence or landslides if permafrost thaws. The primary inputs into the model were vegetation, slope orientation, slope steepness, and a mosaic of the most detailed surficial geology available at the time (including a preliminary version of this surficial geology map).

Permafrost features are only identified on the appended surficial geology map where confirmed in the field or inferred based on obvious signs of permafrost degradation visible in historical imagery. Polygons showing evidence of permafrost processes are identified by the process modifier "-X", whereas landforms indicative of the presence of permafrost are symbolized by line or point features. These include landforms such as thermokarst ponds (Fig. 49), permafrost mounds (lithalsas and palsas; Fig. 50), tension cracks, and permafrost-related landslides such as active-layer detachment failures and retrogressive thaw flows.



**Figure 49.** Thermokarst ponds are abundant in the Ibex Valley agricultural area, and are an excellent indicator of degrading ice-rich permafrost (17DA01-17DA04).



**Figure 50.** Permafrost mound in lower Cowley Creek wetland (20PL017). Leaning (drunken) trees indicate degrading permafrost.

## Flooding

Flooding is a serious concern in terms of both inundation and shoreline erosion in a number of locations around the greater Whitehorse area, particularly along the shorelines of the Yukon and Takhini rivers, Lake Laberge, and Marsh Lake. A record flood season occurred in summer 2021, associated with high snowpack conditions during the previous winter. Previous record flood levels occurred in summer 2007. The 2021 flooding situation prompted Yukon government to declare a state of emergency from July 9 to September 14, and the Canadian Armed Forces was recruited to assist with emergency response efforts.

The record flood level on Marsh Lake was a 1 in 160-year event and reached 657.88 m (CGVD2013 datum)/657.57 m (CGVD28 datum<sup>4</sup>) on July 11, 2021 (Morrison Hershfield, 2022a,b). In comparison, the previous record flood level was a 1 in 50-year event that reached 657.66 m (CGVD2013 datum)/657.34 m (CGVD28 datum) on August 14, 2007 (Morrison Hershfield, 2022a,b).

The record flood level on Lake Laberge reached 628.01 m (CGVD2013 datum)/627.72 m (CGVD28 datum) on July 16, 2021. The previous record flood level reached 627.57 m (CGVD2013) on August 19, 2007 (Morrison Hershfield, 2022b).

For this project, active floodplains were mapped where evidence of recent inundation existed; however, further flood analysis and modelling was beyond the scope of this project. Unvegetated or sparsely vegetated (e.g., grassy or shrubby) portions of the floodplain were generally considered active, while forested ones were not (Fig. 51). Stantec (2022) produced preliminary flood inundation maps and provided a number of flood mitigation options for the Army Beach and South McClintock Road areas of Marsh Lake. Furthermore, Yukon Environment's Water Resources Branch is currently leading a Territory-wide flood-mapping program to develop flood maps for 14 flood-prone communities to be completed over the next several years. The first study, which began in November 2022, specifically targets the Southern Lakes area (which includes Marsh Lake and Lake Laberge, but not the city of Whitehorse); preliminary results are expected by late 2023.



**Figure 51.** Yukon River in flood near Whistle Bend, August 14, 2021.

---

<sup>4</sup> CGVD28 (Canadian Geodetic Vertical Datum 1928) is the datum used for the 2013 to 2019 lidar products that were used for mapping in this project. New lidar acquisitions have transitioned to the CGVD2013 datum.

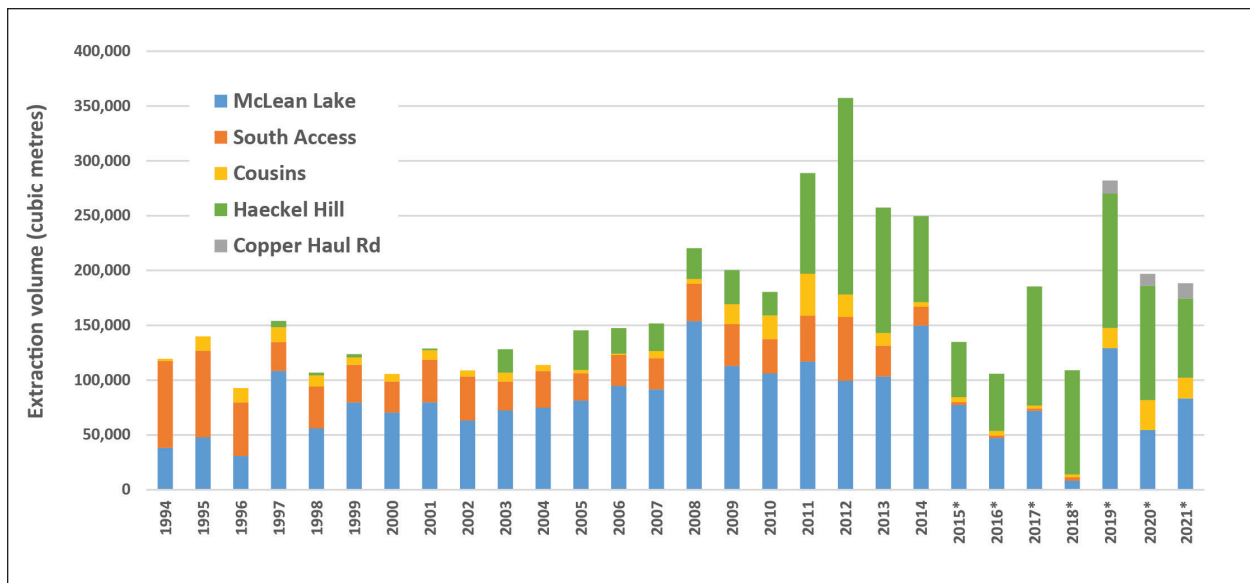


## Aggregate

Aggregate or granular (gravel and sand) resources are vital for supporting ongoing municipal growth, housing developments, and infrastructure construction within the greater Whitehorse area. However, undeveloped reserves that are located within appropriate municipal zoning and acceptable haul distances, and have separation from existing residential areas, are currently very limited.

Annual aggregate extraction in the Whitehorse area fluctuated from approximately 100 000 to 350 000 m<sup>3</sup>/year between 1994 and 2014 (Fig. 52). Key extraction areas within city limits have included the McLean Lake (Fig. 53), Ear Lake (South Access Rd.), Haeckel Hill (Fig. 54), and Cousins airstrip (Fig. 55) areas. Inukshuk (2015) estimated that remaining reserves in active quarries in the McLean Lake and South Access Rd. areas were approximately 9.5 million m<sup>3</sup>, which would be expected to last until about 2050, assuming an average annual extraction rate of 250 000 m<sup>3</sup>/yr. Stevens Quarry and the Whitehorse Tank Farm area also contain large aggregate resources. Various aggregate studies that have been completed in the greater Whitehorse area are summarized in Table 6.

The highest quality aggregate resources are located within glaciofluvial outwash and kame (ice-contact) deposits, often near the mouths of large meltwater channels (e.g., Fig. 54). These landforms are easily identified on the appended surficial geology maps, which provide a critical data source for modelling aggregate potential, as described below. A draft version of this mapping was also shared with the City of Whitehorse in fall of 2022 to inform the 2040 Official Community Plan.



**Figure 52.** Annual aggregate extraction volumes from active Whitehorse quarry leases in primary aggregate areas. Data sources: 1994–2014 from Inukshuk (2015); \*2015–2021 values were self-reported by lease holders to Energy Mines and Resources’ Lands Branch and are incomplete for the McLean Lake area in 2018.



**Figure 53.** McLean Lake quarry pit (September 2020).



**Figure 54.** Thick deposits of glaciofluvial gravel exposed in Castle Rock quarry pits, near Haeckel Hill.



**Figure 55.** Yellow Truck Excavating sand quarry, located near Cousins Airstrip.

**Table 6.** Major aggregate studies conducted in the Whitehorse area in recent decades.

<b>Greater Whitehorse</b>	
R.M. Hardy and Associates, 1978	Whitehorse gravel survey, Alaska Highway and Mayo Road
EBA, 1991c	Whitehorse granular inventory, Whitehorse area
Hoggan, 1995	Granular investigation, greater Whitehorse inventory of sand and gravel reserves
Mollard, 2008	Office airphoto study mapping granular prospects along M'Clintock Valley Road, km 0.0 to km 14.0
Laxton and Coates, 2015	Geophysical and borehole investigation of aggregate resources in the Whitehorse area
Golder Associates, 2015	Geophysical and geological exploration for aggregate in the City of Whitehorse area
Lee <i>et al.</i> , 2017	Near-surface geophysical investigation of a gravel site near Whitehorse
<b>McLean Lake Quarry</b>	
J.R. Paine and Associates, 1988	Quarry gravel investigation, McLean Lake, Whitehorse
Inukshuk, 2015	McLean Lake Quarry assessment
<b>Stevens Quarry</b>	
EBA, 1991a	Geotechnical report, MacPherson Area "A" granular resources
EBA, 1991b	Geotechnical report, MacPherson Area "B" granular resources
EBA, 2011a	Geotechnical evaluation. <i>In:</i> Stevens Quarry Development Plan Update, YESAB project proposal (Appendix 3)
EBA, 2011b	Stevens Quarry sonic drill program. <i>In:</i> Stevens Quarry Development Plan Update, YESAB project proposal (Appendix 4)
Inukshuk, 2012	Stevens Quarry development plan, update 2012

### Aggregate potential analysis

Aggregate potential analysis was completed using this most recent surficial geology mapping to identify potential near-surface aggregate resources. This analysis focussed specifically on the gravel size class, and did not include sand, boulder or bedrock quarrying potential. The model inputs included surficial material type, texture, surface expression, and relative proportions of the two most dominant surficial geology components (MATERIAL A and MATERIAL B) mapped within each polygon.

The analysis followed a similar approach to that outlined by Cronmiller (2021), with modifications for ranking specific combinations of surficial materials, textures and surface expressions, which are more likely to contain high-quality aggregate resources. Weightings were applied to incorporate relative abundance of gravel indicated in the material texture, and the relative thickness of the deposit (e.g., veneers were weighted less than thicker surface expressions).

The highest ranked materials are glaciofluvial materials (FG), followed by inactive fluvial materials (F) and hummocky moraine deposits (gMh; Table 7). Despite their high potential material suitability, active fluvial materials (FA) are ranked low, as they are assumed impractical for development due to high-water tables and environmental concerns. Organic (O), bedrock (R), and fine-grained lacustrine (L, LG) and eolian (E) materials are also ranked low. Colluvial (C) and other morainal (M) deposits are generally ranked moderate with weightings applied based on texture and surface expression. Rankings for anthropogenic (A) materials vary according to the nature of the materials (Table 7). Aggregate potential is lowered where the presence of permafrost is indicated, or if a deposit is buried and would require surface stripping. Where larger deposits are present, the relative cost of stripping or thawing may be low, so the aggregate potential scores should be viewed as subjective in this respect.

Overall aggregate potential was calculated using the following equations:

$$\text{Aggregate Potential Score} = \text{Material Suitability} - (0.25 \times \text{Stripping Value}) - (0.25 \times \text{Permafrost Value})$$

where

$$\text{Material Suitability} = \text{Max Value } ((\text{Material A Proportion} \times \text{Material A Suitability}) \text{ or } (\text{Material B Proportion} \times \text{Material B Suitability}))$$

A summary of values used for the variables above is provided in Table 8.

Final aggregate potential scores ranged from 0 to 3 (0 being the lowest and 3 being the highest potential); these were then assigned to the qualitative aggregate classes, as outlined in Table 8. Only the high (H) and moderate-high (MH) classes (Fig. 56 and Sheet 11) are considered potentially viable as aggregate resources; lower classes would likely require a significant amount of washing and/or screening to recover any useful granular resources. Eskers (line features shown on Sheet 11) may also provide small, but high-quality aggregate resources.

High aggregate potential materials typically consist of well-sorted gravel with some sand, minimal silt and clay, and minor to no constraints from permafrost or overburden. Moderately high aggregate potential materials consist of (a) good aggregate materials, as described above, but may be thinner and/or have a greater sand content, and/or are constrained by significant overburden or permafrost; or (b) gravel mixed with some silt and/or clay, but not subject to significant constraints from permafrost or overburden.

## Limitations

The final aggregate classes serve as a general guide to aggregate potential only, as they are based on the characteristics of the mapped surficial geology, which may vary significantly within a polygon, and for which limited field verification has occurred. Site-specific field investigations such as test pitting and/or drilling would be required to determine thickness, volume, and exact composition. The analysis does not take into account factors that may limit the feasibility of extraction, including existing land tenure, municipal zoning, topographic constraints, presence of mass movements, or proximity to roads, communities or water features.

**Table 7.** Material suitability values assigned to various surficial material types.

<b>Glaciofluvial (FG)</b>		<b>Colluvium (C)</b>	
g__FG	3	(d,g, or x)__C(f,a)	2
g__FGv	2	_(g,d or x)_C(f,a)	1.5
_g__FG	2.5	(d,g or x)_C(≠f,a)	1.5
_g__FGv	1.5	(≠d,g or x)dC(≠f,a)	0.5
other FG (no g)	1	(≠d,g or x)_C(≠f,a)	0.1
<b>Fluvial, inactive (F)</b>		<b>Lacustrine (L)</b>	
g__F	2.5	gg_Lr	2
g__Fv	1.5	(≠g)_L	0.1
_g__F	2	<b>Eolian (E)</b>	
__gF	1.5	s(≠z)_E	1
__gFv	1	all other E	0.1
other F (no g)	0.5	<b>Bedrock (R)</b>	
<b>Fluvial, active (FA)</b>		0	
g__FA	1	<b>Anthropogenic (A)</b>	
_g__FA	0.5	road fill	3
other FA (no g)	0.1	urban	2
<b>Morainal (M)</b>		mine waste	2
g__Mh	3	mine tailings	0
dgM (≠h)	1.5	landfill, lagoon	0
(≠d,g__)M (≠h)	1	berm, dyke	0
<b>Organic (O)</b>		<b>Water Bodies (H)</b>	
0		0	

Notes: Up to three textures may be assigned to a surficial geology component, and are represented by lower case letters listed before upper case surficial material symbols, in order of decreasing abundance (i.e., g\_\_ > \_g\_ > \_\_g). 'Wild' value place markers are represented by underscore symbols. g = gravel (rounded fragments >2mm), d = mixed angular/round fragments > 2mm, x = angular fragments >2mm, s = sand. Surface expression is represented by lower case letter immediately following upper case surficial material symbols: h = hummocky, f = fan, a = apron, v = veneer (<1 m thick), r = ridge.

**Table 8.** Values used for various aggregate potential scoring variables.

<b>Stripping Value (0.25)</b>		
<i>where (RELATIONAB = '\')</i> AND (Material A suitability < Material A suitability) AND...		
Material A surface expression = 'v' or 'x'	1	
Material A surface expression = 'b'	2	
Material A surface expression = other	3	
<b>Permafrost Value (0.25)</b>		
Indicated (-X)	1	
Not indicated	0	
<b>Material A Proportion</b>		
Partial cover ('/')	0.5	
Full cover	1	
<b>Material B Proportion</b>		
RELATIONAB = null	0	
RELATIONAB = '.'	0.5	
RELATIONAB = '.' AND RELATIONBC = '/'	0.35	
RELATIONAB = '.' AND RELATIONBC = '//'	0.45	
RELATIONAB = '/' AND RELATIONBC = ''	0.3	
RELATIONAB = '/' AND RELATIONBC = '.'	0.15	
RELATIONAB = '/' AND RELATIONBC = '/'	0.21	
RELATIONAB = '/' AND RELATIONBC = '//'	0.27	
RELATIONAB = '/' AND RELATIONBC = '\'	0.3	
RELATIONAB = '//'	0.15	
RELATIONAB = '\'	1	
RELATIONAB = '\'	0.5	
RELATIONAB = '\'	0.7	
RELATIONAB = '\'	0.9	
<b>Aggregate Potential Class</b>		
Aggregate Potential Score <= 0.5	VL	Very Low
Aggregate Potential Score = > 0.5 - 1	L	Low
Aggregate Potential Score = > 1 - 1.5	LM	Low - Moderate
Aggregate Potential Score = > 1.5 - 2	M	Moderate
Aggregate Potential Score = > 2 - 2.5	MH	Moderate - High
Aggregate Potential Score = > 2.5 - 3	H	High

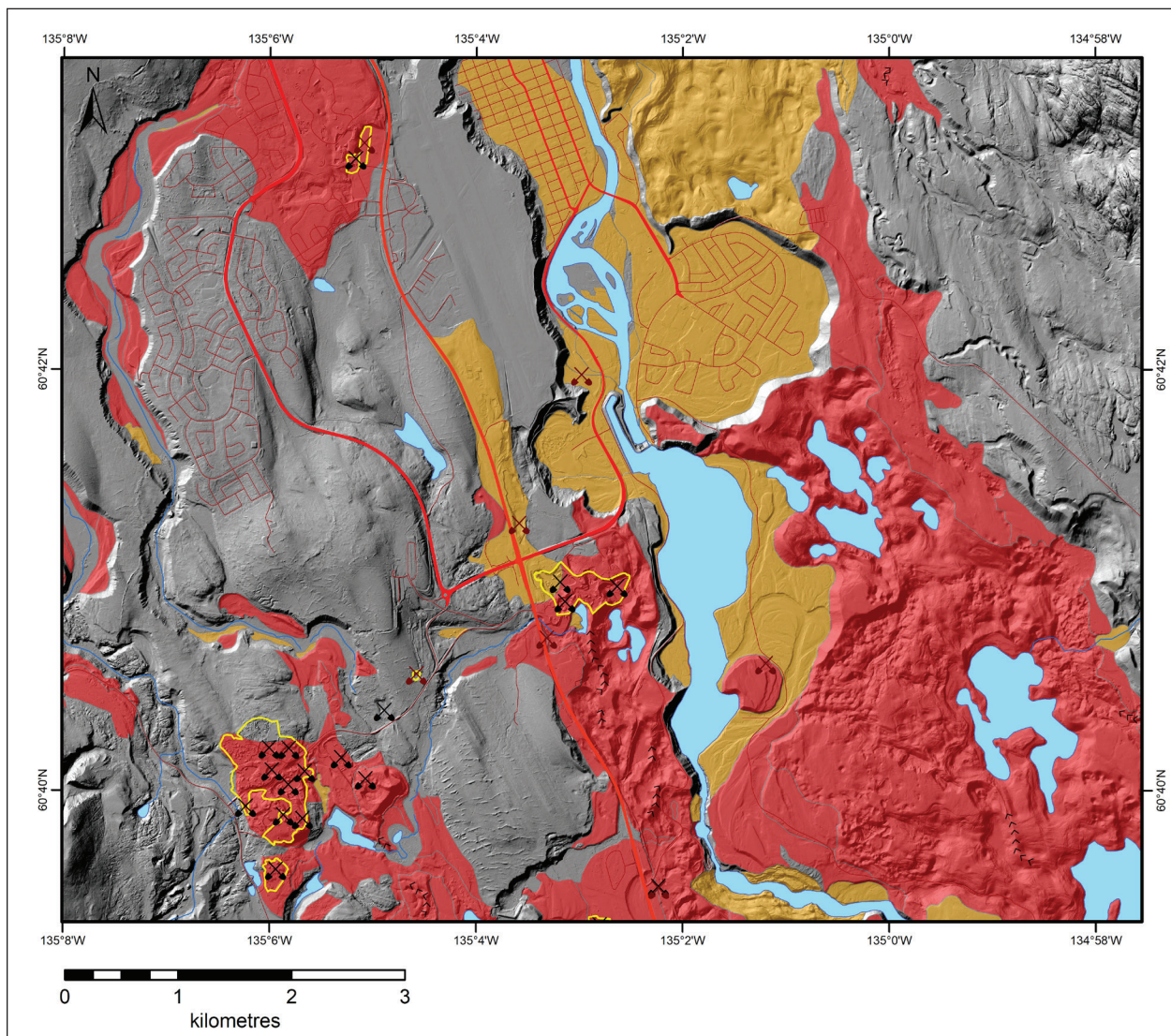
Notes: RELATIONAB and RELATIONBC refer to field names in the surficial geology polygon attribute table, which describe relative abundance of components A vs B or B vs C within a polygon.

'.' indicates that both components (e.g., A and B) are found in roughly equal proportions

'/' indicates that the first component (e.g., A) is more extensive than the second (e.g., B)

'//' indicates that the first component (e.g., A) is much more extensive than the second (e.g., B)

'\'



**Figure 56.** Extract of aggregate potential map for south access (Ear Lake) and McLean Lake areas. Red and orange areas have high and moderately high aggregate potential, respectively. Yellow lines outline active and historical gravel pits. Refer to Sheet 11 for complete map encompassing Whitehorse city limits.

## Acknowledgements

This project was carried out on the traditional territories of the Kwanlin Dün First Nation, Ta'an Kwäch'än Council, and Champagne and Aishihik First Nations. Exceptional field assistance was provided by Amaya Cherian-Hall, Emilie Stewart-Jones, Moya Painter and Jennifer Humphries. Thanks to Michael Kishchuk (Dalhousie University) and Brad Harvey (Geological Survey of Canada) for their tremendous contributions toward investigating soil gas radon in the study area. During investigations of the 2022 Whitehorse escarpment landslides, support was greatly appreciated from Taylor Eshpeter, Michael Abbott and Tracy Allen from the City of Whitehorse, and Brendan Mulligan from Yukon Water Resources Branch. Much gratitude to Jeff Bond, Maurice Colpron and Derek Cronmiller for their thoughtful and thorough reviews of this work, as well as Leyla Weston for editing and Bailey Staffen for layout.

## References

- Barnes, S.D., 1997. The sedimentology and paleogeography of Glacial Lake Champagne, southern Yukon Territory. MA thesis, Carleton University, Ontario, Canada, 109 p.
- Bond, J., 2004. Late Wisconsinan McConnell glaciation of the Whitehorse map area (105D), Yukon. In: Yukon Exploration and Geology 2003, D.S. Emond and L.L. Lewis (eds.), Yukon Geological Survey, p. 73-88. [https://ygsftp.gov.yk.ca/publications/yeg/yeg03/07\\_bond.pdf](https://ygsftp.gov.yk.ca/publications/yeg/yeg03/07_bond.pdf)
- Bond, J.D., Morison, S. and McKenna, K., 2005a. Surficial Geology of Carcross (NTS 105D/02), Yukon. Yukon Geological Survey, Geoscience Map 2005-2, 1:50 000 scale. [https://ygsftp.gov.yk.ca/publications/geoscience\\_map/2005/gm2005\\_2.pdf](https://ygsftp.gov.yk.ca/publications/geoscience_map/2005/gm2005_2.pdf)
- Bond, J.D., Morison, S. and McKenna, K., 2005b. Surficial Geology of Fenwick Creek (NTS 105D/03), Yukon. Yukon Geological Survey, Geoscience Map 2005-3, 1:50 000 scale. [https://ygsftp.gov.yk.ca/publications/geoscience\\_map/2005/gm2005\\_3.pdf](https://ygsftp.gov.yk.ca/publications/geoscience_map/2005/gm2005_3.pdf)
- Bond, J.D., Morison, S. and McKenna, K., 2005c. Surficial Geology of Alligator Lake (NTS 105D/06), Yukon. Yukon Geological Survey, Geoscience Map 2005-4, 1:50 000 scale. [https://ygsftp.gov.yk.ca/publications/geoscience\\_map/2005/gm2005\\_4.pdf](https://ygsftp.gov.yk.ca/publications/geoscience_map/2005/gm2005_4.pdf)
- Bond, J.D., Morison, S. and McKenna, K., 2005d. Surficial Geology of Robinson (NTS 105D/07), Yukon. Yukon Geological Survey. Geoscience Map 2005-5, 1:50 000 scale. [https://ygsftp.gov.yk.ca/publications/geoscience\\_map/2005/gm2005\\_5.pdf](https://ygsftp.gov.yk.ca/publications/geoscience_map/2005/gm2005_5.pdf)
- Bond, J.D., Morison, S. and McKenna, K., 2005e. Surficial Geology of MacRae (NTS 105D/10), Yukon. Yukon Geological Survey, Geoscience Map 2005-6, 1:50 000 scale. [https://ygsftp.gov.yk.ca/publications/geoscience\\_map/2005/gm2005\\_6.pdf](https://ygsftp.gov.yk.ca/publications/geoscience_map/2005/gm2005_6.pdf)
- Bond, J.D., Morison, S. and McKenna, K., 2005f. Surficial geology of Whitehorse (NTS 105D/11). Yukon Geological Survey, Geoscience Map 2005-7, 1:50 000 scale. [https://ygsftp.gov.yk.ca/publications/geoscience\\_map/2005/gm2005\\_7.pdf](https://ygsftp.gov.yk.ca/publications/geoscience_map/2005/gm2005_7.pdf)
- Bond, J., Morison, S. and McKenna, K., 2005g. Surficial Geology of Upper Laberge (NTS 105D/14), Yukon. Yukon Geological Survey, Geoscience Map 2005-8, 1:50 000 scale. [https://ygsftp.gov.yk.ca/publications/geoscience\\_map/2005/gm2005\\_8.pdf](https://ygsftp.gov.yk.ca/publications/geoscience_map/2005/gm2005_8.pdf)
- Bordet, E., 2019. Bedrock geology map of the eastern Lake Laberge area (parts of NTS 105E/2,3,6,7 and 105D/15,16). Yukon Geological Survey, Geoscience Map GM2019-1, scale 1:50 000, 2 sheets. <https://data.geology.gov.yk.ca/Reference/81635#InfoTab>
- Bordet, E., Crowley, J.L. and Piercey, S.J., 2019. Geology of eastern Lake Laberge area (105E), south-central Yukon. Yukon Geological Survey, Open File 2019-1, 120 p. <https://data.geology.gov.yk.ca/Reference/81653#InfoTab>
- Brideau, M.-A., Stead, D., Bond, J.D., Lipovsky, P.S. and Ward, B.C., 2011. Preliminary stratigraphic and geotechnical investigations of the glaciolacustrine and loess deposits around the city of Whitehorse (NTS 105D/11), Yukon. In: Yukon Exploration and Geology 2010, K.E. MacFarlane, L.H. Weston and C. Relf (eds.), Yukon Geological Survey, p. 33-53. [https://ygsftp.gov.yk.ca/publications/yeg/yeg10/YEG/04\\_Brideau\\_etal.pdf](https://ygsftp.gov.yk.ca/publications/yeg/yeg10/YEG/04_Brideau_etal.pdf)
- Calmels, F., Roy, L.P., Laurent, C., Amyot, F. and Lipovsky, P., 2021. Assessment and monitoring of a new retrogressive thaw slump at km 1456 of the Alaska Highway: A rare opportunity. Yukon University Research Centre, 72 p. [https://www.yukonu.ca/sites/default/files/inline-files/PGR\\_2021\\_01\\_Tak\\_Slump\\_NTAI\\_0.pdf](https://www.yukonu.ca/sites/default/files/inline-files/PGR_2021_01_Tak_Slump_NTAI_0.pdf)



- Colpron, M. (comp.), 2011. Geological compilation of Whitehorse trough - Whitehorse (105D), Lake Laberge (105E), and part of Carmacks (115I), Glenlyon (105L), Aishihik Lake (115H), Quiet Lake (105F) and Teslin (105C) (1:250 000-scale). Yukon Geological Survey, Geoscience Map 2011-1, 3 maps, legend and appendices. <https://data.geology.gov.yk.ca/Reference/50370#InfoTab>
- Colpron, M., Crowley, J.L., Gehrels, G.E., Long, D.G.F., Murphy, D.C., Beranek, L.P. and Bickerton, L., 2015. Birth of the northern Cordilleran orogen, as recorded by detrital zircons in Jurassic synorogenic strata and regional exhumation in Yukon. *Lithosphere*, vol. 7, p. 541-562.
- Colpron, M., Sack, P.J., Crowley, J.L., Beranek, L.P. and Allan, M.M., 2022. Late Triassic to Jurassic magmatic and tectonic evolution of the Intermontane terranes in Yukon, northern Canadian Cordillera: Transition from arc to syn-collisional magmatism and post-collisional lithospheric delamination. *Tectonics*, vol. 41, doi: 10.1029/2021TC007060.
- Cronmiller, D.C., 2021. Aggregate potential mapping centred on Yukon communities and highway corridors. Yukon Geological Survey, Open File 2021-3, 6 pages plus appendices. <https://data.geology.gov.yk.ca/Reference/95907#InfoTab>
- Eberle, J., Hutchison, J.H., Kennedy, K., Koenigswald, W., MacPhee, R.D.E. and Zazula, G.D., 2019. The first Tertiary fossils of mammals, turtles, and fish from Canada's Yukon. In: *American Museum Novitates*, no. 3943, 28 p. <https://digitallibrary.amnh.org/bitstream/handle/2246/6967/N3943.pdf?sequence=1&isAllowed=y>
- EBA Engineering Consultants Ltd., 1991a. Geotechnical report, MacPherson Area "A" granular resources, Whitehorse, Yukon. Submitted to Government of Yukon, Department of Community and Transportation, Lands Branch.
- EBA Engineering Consultants Ltd., 1991b. Geotechnical report, MacPherson Area "B" granular resources, Whitehorse, Yukon.
- EBA Engineering Consultants Ltd., 1991c. Whitehorse granular inventory, Whitehorse area, Whitehorse, Yukon. Submitted to Government of Yukon.
- EBA Engineering Consultants Ltd., 2002. Geohazard risk study, Whitehorse Escarpment. Prepared for City of Whitehorse, October, 2002.
- EBA Engineering Consultants Ltd., 2011a. Appendix 3, Geotechnical evaluation. In: Stevens Quarry Development Plan Update, YESAB project proposal.
- EBA Engineering Consultants Ltd., 2011b. Appendix 4, Stevens Quarry sonic drill program. In: Stevens Quarry Development Plan Update, YESAB project proposal.
- EBA Engineering Consultants Ltd., A Tetra Tech Company (EBA), 2012. Downtown south terrain stability assessments. Prepared for City of Whitehorse – Engineering and Environment.
- EBA Engineering Consultants Ltd., A Tetra Tech Company (EBA), 2014. Preliminary aquifer and wellhead protection plan, Takhini River subdivision, Yukon. Prepared for Champagne Aishihik First Nation.
- Environment Yukon, 2022. Yukon water well registry. Water Resources Branch, <https://yukon.maps.arcgis.com/apps/webappviewer/index.html?id=51322dfb133d42c4ad184fee9986048b> [accessed on Dec. 1, 2022].
- Eyles, N., Eyles, C. W., Lau, K. and Clark, B., 1985. Applied Sedimentology in an Urban Environment — the Case of Scarborough Bluffs, Ontario: Canada's Most Intractable Erosion Problem. *Geoscience Canada*, vol. 12, no. 3, p. 91–104. [https://www.erudit.org/en/journals/geocan/1985-v12-n3-geocan\\_12\\_3/geocan12\\_3art01.pdf](https://www.erudit.org/en/journals/geocan/1985-v12-n3-geocan_12_3/geocan12_3art01.pdf)

- Gartner Lee Ltd., 2003. Preliminary groundwater inventory of the City of Whitehorse. Prepared for: Community Development Branch, Department of Community Services, Government of Yukon. 53 p + 8 x 1:50 000 scale maps. [https://emrlibrary.gov.yk.ca/cs/upper\\_yukon\\_river\\_groundwater\\_inventory\\_2001/Whitehorse%20Groundwater%20Inventory.pdf](https://emrlibrary.gov.yk.ca/cs/upper_yukon_river_groundwater_inventory_2001/Whitehorse%20Groundwater%20Inventory.pdf)
- Gilbert, R. and Desloges, J.R., 2005. The record of Glacial Lake Champagne in Kusawa Lake, southwest Yukon Territory. *Canadian Journal of Earth Sciences*, vol. 42, p. 2127-2140.
- Golder Associates, 2015. Geophysical and geological exploration for aggregate in the City of Whitehorse area. Yukon Geological Survey, Miscellaneous Report MR-12, 68 p. [https://ygsftp.gov.yk.ca/publications/miscellaneous/Reports/MR\\_12/MR-12.pdf](https://ygsftp.gov.yk.ca/publications/miscellaneous/Reports/MR_12/MR-12.pdf)
- Hart, C.J.R. and Radloff, J.K., 1990. Geology of Whitehorse, Alligator Lake, Fenwick Creek Carcross and Part of Robinson Map Areas (105D/11, 6, 3, 2 & 7). Yukon Geological Survey, Open File 1990-4(G). <https://data.geology.gov.yk.ca/Reference/42405#InfoTab>
- Hart, C.J.R., 1997a. A Transect Across Northern Stikinia: Geology of the Northern Whitehorse Map Area, Southern Yukon Territory (105D/13-16). Exploration and Geological Services Division, Yukon, Indian and Northern Affairs Canada, Bulletin 8, 112 p. <https://ygsftp.gov.yk.ca/publications/bulletin/bulletin8.pdf>
- Hart, C.J.R., 1997b. Geology of Thirty-seven Mile Creek map area, southern Yukon Territory, (NTS 105D/13). Indian and Northern Affairs Canada/Department of Indian and Northern Development: Exploration and Geological Services Division, Geoscience Map 1997-4. [https://ygsftp.gov.yk.ca/publications/geoscience\\_map/1997/gm1997\\_4.pdf](https://ygsftp.gov.yk.ca/publications/geoscience_map/1997/gm1997_4.pdf)
- Hart, C.J.R., 1997c. Geology of Upper Laberge Map Area, Southern Yukon (NTS 105D/14). Indian & Northern Affairs Canada/Department of Indian & Northern Development: Exploration & Geological Services Division, Geoscience Map 1997-5. [https://ygsftp.gov.yk.ca/publications/geoscience\\_map/1997/gm1997\\_5.pdf](https://ygsftp.gov.yk.ca/publications/geoscience_map/1997/gm1997_5.pdf)
- Hart, C.J.R., 1997d. Geology of Mount M'Clintock Map Area, Southern Yukon (NTS 105D/16). Indian & Northern Affairs Canada/Department of Indian & Northern Development: Exploration & Geological Services Division, Geoscience Map 1997-7. [https://ygsftp.gov.yk.ca/publications/geoscience\\_map/1997/gm1997\\_7.pdf](https://ygsftp.gov.yk.ca/publications/geoscience_map/1997/gm1997_7.pdf)
- Hart, C.J.R. and Hunt, J.A., 1997. Geology of Joe Mountain map area, southern Yukon Territory, 1:50 000-scale map (105D/15). Exploration and Geological Services Division, Yukon, Indian and Northern Affairs Canada, Geoscience Map 1997-6. [https://ygsftp.gov.yk.ca/publications/geoscience\\_map/1997/gm1997\\_6.pdf](https://ygsftp.gov.yk.ca/publications/geoscience_map/1997/gm1997_6.pdf)
- Hart, C.J.R. and Villeneuve, M., 1999. Geochronology of Neogene alkaline volcanic rocks (Miles Canyon basalt), southern Yukon Territory, Canada: The relative effectiveness of laser  $^{40}\text{Ar}/^{39}\text{Ar}$  and K-Ar geochronology. *Canadian Journal of Earth Sciences*, vol. 36, p. 1495-1507. <https://doi.org/10.1139/e99-049>
- Heffner, T., 2008. The role of glacial lakes in the pre-contact human history of southwest Yukon Territory: a late drainage hypothesis. *The Northern Review*, vol. 29, p. 85-104.
- Heginbottom, J.A., 1995. National Atlas of Canada (5th edition), Canada Permafrost, Plate 2.1 (MCR 4177), 1:7 500 000 scale.
- Heon, D. and Hart, C.J.R., 1998. Mineral Potential Map of the City of Whitehorse. Exploration and Geological Services Division, Yukon, Indian and Northern Affairs Canada, Open File 1998-6 (1:30 000-scale). <https://ygsftp.gov.yk.ca/publications/openfile/1998/of1998-6.pdf>
- Heon, D., 2004. The Whitehorse Copper Belt - An annotated geology map. Yukon Geological Survey, Open File 2004-15. <https://data.geology.gov.yk.ca/Reference/42284#InfoTab>

- Heon, D., Bond, J., Gilbert, G., Tenney, D., Pearson, F., Stroshein, R., Stuart, A., Roots, C. and Pelletier, K., 2004. The Whitehorse Copper Belt, Yukon: A booklet to accompany YGS OF 2004-15. Yukon Geological Survey, 20 p. [https://ygsftp.gov.yk.ca/publications/brochures/copperbelt\\_booklet.pdf](https://ygsftp.gov.yk.ca/publications/brochures/copperbelt_booklet.pdf)
- Hoggan Engineering and Testing Ltd., 1995. Granular investigation, greater Whitehorse inventory of sand and gravel reserves, Whitehorse, Yukon.
- Horton, S., 2007. The Paleogeography of Glacial Lake Laberge, south central Yukon Territory. Unpublished BSc Honours thesis, University of Victoria, British Columbia, Canada, 53 p.
- Howes, D.E. and Kenk, E., 1997. Terrain classification system for British Columbia, version 2. Resource Inventory Branch, Ministry of Environment, Lands and Parks, 112 p. [https://www2.gov.bc.ca/assets/gov/environment/natural-resource-stewardship/nr-laws-policy/risc/terclass\\_system\\_1997.pdf](https://www2.gov.bc.ca/assets/gov/environment/natural-resource-stewardship/nr-laws-policy/risc/terclass_system_1997.pdf)
- Hungr, O., Leroueil, S. and Picarelli, L., 2014. The Varnes classification of landslide types, an update. *Landslides*, vol. 11, p. 167-194. DOI 10.1007/s10346-013-0436-y. <https://link.springer.com/article/10.1007/s10346-013-0436-y>
- Huscroft, C.A., Lipovsky, P.S. and Bond, J.D., 2004. A regional characterization of landslides in the Alaska Highway corridor, Yukon. Yukon Geological Survey, Open File 2004-18. <https://data.geology.gov.yk.ca/Reference/42286#InfoTab>
- Inukshuk Planning and Development, 2012. Stevens Quarry development plan, update 2012.
- Inukshuk Planning and Development, 2015. McLean Lake Quarry assessment, June 2015.
- J.R. Paine and Associates Ltd., 1988. Quarry gravel investigation (1988), McLean Lake, Whitehorse, Yukon Territory.
- Keefer, D.K., 1984. Landslides caused by earthquakes. *Geological Society of America Bulletin*, vol. 95, p. 406-421.
- Keefer, D.K., 2002. Investigating landslides caused by earthquakes – a historical review. *Surveys in Geophysics*, vol. 23, p. 473-510.
- Kishchuk, M.J., Lipovsky, P.S., Bond, J.D. and Gosse, J.C., 2021. Preliminary investigation of geological controls on radon concentration in surficial sediment in Whitehorse, Yukon (NTS 105D/11, 14). In: *Yukon Exploration and Geology 2020*, K.E. MacFarlane (ed.), Yukon Geological Survey, p. 115–135. <https://data.geology.gov.yk.ca/Reference/95899#InfoTab>
- Kishchuk, M.J., 2021. Geological controls on radon concentration in surficial sediment in Whitehorse, Yukon. Unpublished BSc Honours thesis, Dalhousie University, Nova Scotia, Canada, 68 p. <https://emrlibrary.gov.yk.ca/theses/kishchuk-m-2021.pdf>
- Klassen, R.W., 1978. Surficial Geology, Takhini River, Yukon Territory. GSC OF539 (Map 1), 1:100 000 scale.
- Klassen, R.W. and Morison, S.R., 1987. Surficial geology, Laberge, Yukon Territory. GSC Map 8-1985, 1:250 000 scale.
- Laxton, S. and Coates, J., 2015. Geophysical and borehole investigation of aggregate resources in the Whitehorse area, Yukon. Yukon Geological Survey, Open File 2015-1, 24 p. <https://ygsftp.gov.yk.ca/publications/openfile/2015/OF2015-1.pdf>
- Lee, Y.K, Bank, C.-G. and Laxton, S., 2017. Near-surface geophysical investigation of a gravel site near Whitehorse, Yukon. In: *Yukon Exploration and Geology 2016*, K.E. MacFarlane and L.H. Weston (eds.), Yukon Geological Survey, p. 141-148. [https://ygsftp.gov.yk.ca/publications/yeg/yeg16/papers/7\\_Lee\\_etal.pdf](https://ygsftp.gov.yk.ca/publications/yeg/yeg16/papers/7_Lee_etal.pdf)

- Leggett, R.F. and Johnston, G.H., 1959. The Whitehorse Escarpment. National Research Council, Report 136. Division of Building Research. <https://doi.org/10.4224/20386566>
- Lipovsky, P.S., Humphries, J.K., Stewart-Jones, E.T. and Cronmiller, D.C., 2022. Yukon Permafrost Database: A new baseline data resource. In: Yukon Exploration and Geology 2021, K.E. MacFarlane (ed.), Yukon Geological Survey, p. 37–49. [https://ygsftp.gov.yk.ca/publications/yeg/yeg2021/papers/3\\_Lipovsky\\_et al.pdf](https://ygsftp.gov.yk.ca/publications/yeg/yeg2021/papers/3_Lipovsky_et al.pdf)
- Long, D.G.F., 2005. Sedimentology and hydrocarbon potential of fluvial strata in the Tantalus and Aksala formations, northern Whitehorse Trough, Yukon. In: Yukon Exploration and Geology 2004, D.S. Emond, L.L. Lewis and G.D. Bradshaw (eds.), Yukon Geological Survey, p. 167–176. [https://ygsftp.gov.yk.ca/publications/yeg/yeg04/12\\_long.pdf](https://ygsftp.gov.yk.ca/publications/yeg/yeg04/12_long.pdf)
- Menounos, B., Goehring, B.M., Osborn, G., Margold, M., Ward, B., Bond, J., Clarke, G.K.C., Clague, J.J., Lakeman, T., Koch, J., Caffee, M.W., Gosse, J., Stroeven, A.P., Seguinot, J. and Heyman, J., 2017. Cordilleran Ice Sheet mass loss preceded climate reversals near the Pleistocene Termination. *Science*, vol. 358, p. 781–784.
- Mollard, 2008. Office airphoto study mapping granular prospects along M'Clintock Valley Road, km 0.0 to km 14.0, Yukon.
- Monahan, P.A., Levson, V.M., Henderson, P. and Sy, A., 2000. Relative liquefaction and amplification of ground motion hazard maps of Greater Victoria. British Columbia Geological Survey, Geoscience Map 2000-3.
- Morison, S.R. and Klassen, R.W., 1991. Surficial geology, Whitehorse, Yukon Territory. GSC Map 12-1990, 1:250 000 scale.
- Morison, S., McKenna, K. and Davies, S., 1982a. 105D NE Surficial Geology and Soils (Southern Lakes Project). Yukon Government unpublished, 1:100 000 scale.
- Morison, S., McKenna, K. and Davies, S., 1982b. 105D NW Surficial Geology and Soils (Southern Lakes Project). Yukon Government unpublished, 1:100 000 scale.
- Morison, S., McKenna, K. and Davies, S., 1982c. 105D SE Surficial Geology and Soils (Southern Lakes Project). Yukon Government unpublished, 1:100 000 scale.
- Morison, S., McKenna, K. and Davies, S., 1982d. 105D SW Surficial Geology and Soils (Southern Lakes Project). Yukon Government unpublished, 1:100 000 scale.
- Morrison Hershfield, 2022a. Updated flood frequency analysis for Southern Lakes. Memorandum submitted to Yukon Government Department of Environment, Water Resources Branch, 13 January 2022.
- Morrison Hershfield, 2022b. Water level-return period relationships for rivers and lakes in Yukon – 2022 update. Memorandum submitted to Yukon Government Community Services, Infrastructure Development Branch, October 2022.
- Mougeot, C.M. and Smith, C.A.S., 1992. Soils of the Whitehorse area, Takhini Valley, Yukon Territory In: Soil Survey Report No. 2. Agriculture Canada. 3 x 1:20 000 scale map sheets <https://sis.agr.gc.ca/cansis/publications/surveys/yt/yt02/index.html>. (Detailed soil survey GIS compilation dataset: [https://sis.agr.gc.ca/cansis/nsdb/dss/v3/dss\\_v3\\_yt\\_20140225.zip](https://sis.agr.gc.ca/cansis/nsdb/dss/v3/dss_v3_yt_20140225.zip) [accessed on Dec. 1, 2022].)
- Mougeot, C.M. and Smith, C.A.S., 1994. Soils of the Whitehorse area, Carcross Valley, Yukon Territory In: Soil Survey Report No. 2. Agriculture Canada. 2 x 1:20 000 scale map sheets. Detailed soil survey compilation dataset, Whitehorse area, 1:20 000 scale: <https://sis.agr.gc.ca/cansis/publications/surveys/yt/yt02/index.html>. (Detailed soil survey GIS compilation dataset: [https://sis.agr.gc.ca/cansis/nsdb/dss/v3/dss\\_v3\\_yt\\_20140225.zip](https://sis.agr.gc.ca/cansis/nsdb/dss/v3/dss_v3_yt_20140225.zip) [accessed on Dec. 1, 2022].)

- Mougeot, C.M., 1994. Preliminary assessment of the clay deposits in selected areas of the Whitehorse map sheet area (105D) for the manufacture of clay based products. Mougeot GeoAnalysis, Whitehorse, Yukon, unpublished report prepared for the Yukon-Canada Co-operation Agreement for Small Business, 57 p.
- Mougeot GeoAnalysis, 1997. Soil, terrain, and wetland survey of the City of Whitehorse. Unpublished draft report (160 p.) with 1:20 000 scale map, prepared by Mougeot GeoAnalysis and Agriculture and Agri-food Canada, for Planning Services, City of Whitehorse, May 1997. [https://sis.agr.gc.ca/cansis/publications/surveys/yt/ytw/ytw\\_report.pdf](https://sis.agr.gc.ca/cansis/publications/surveys/yt/ytw/ytw_report.pdf)
- Mougeot, C.M., 1998. Soil and terrain features of the Yukon River corridor, City of Whitehorse, Yukon. Unpublished report (29 p.) with maps at 1:40 000 scale, prepared by Mougeot GeoAnalysis for Gartner Lee Environmental Consultants Ltd., Sept. 1998.
- Mougeot, C.M. and Smith, C.A.S., 1998. Terrain and surficial geology of the City of Whitehorse, Yukon Territory, 1:30 000 scale. Produced by Mougeot GeoAnalysis, Agriculture and Agri-food Canada and Gartner Lee Ltd. for City of Whitehorse. [https://sis.agr.gc.ca/cansis/publications/surveys/yt/ytw/ytw\\_map1.zip](https://sis.agr.gc.ca/cansis/publications/surveys/yt/ytw/ytw_map1.zip)
- Mougeot, C.M. and Smith, C.A.S., 1999. Soils of the City of Whitehorse, Yukon Territory, 1:30 000 scale. Produced by Mougeot GeoAnalysis, Agriculture and Agri-food Canada and Gartner Lee Ltd. for City of Whitehorse. [https://sis.agr.gc.ca/cansis/publications/surveys/yt/ytw/ytw\\_map2.zip](https://sis.agr.gc.ca/cansis/publications/surveys/yt/ytw/ytw_map2.zip)
- Natural Resources Canada, 2015. Simplified seismic hazard map for Canada, the provinces and territories. <https://earthquakescanada.nrcan.gc.ca/hazard-alea/simphaz-en.php#YT>, [accessed 2022/12/09].
- Natural Resources Canada, 2022. National earthquake database. <https://earthquakescanada.nrcan.gc.ca/stndon/NEDB-BNDS/index-en.php>, [accessed 2022/12/09].
- Pearson, F.K., Hart, C.J.R. and Power, M., 2001. Distribution of Miles Canyon basalt in the Whitehorse area and implications for groundwater resources. In: Yukon Exploration and Geology 2000, D.S. Emond, and L.W. Weston (eds.), Exploration and Geological Services Division, Yukon, Indian and Northern Affairs Canada, p. 235-245. [https://ygsftp.gov.yk.ca/publications/yeg/yeg00/19\\_pearson.pdf](https://ygsftp.gov.yk.ca/publications/yeg/yeg00/19_pearson.pdf)
- R.M. Hardy and Associates Ltd., 1978. Whitehorse gravel survey, Alaska Highway and Mayo Road.
- Roy, L.-P., Lipovsky, P.S., Calmels, F., Laurent, C., Humphries, J. and Vogt, N., 2021. Greater Whitehorse area permafrost characterization. Yukon Geological Survey, Miscellaneous Report MR-22, 185 p., including appendices. <https://ygsftp.gov.yk.ca/publications/miscellaneous/Reports/MR-22.pdf>
- Stantec, 2022. Marsh Lake flood mitigation options. Prepared for Government of Yukon Community Services, Infrastructure Development Branch. March 22, 2022. [https://yukon.ca/sites/yukon.ca/files/cs/2022-03-24\\_ml-floodmitigationoptionsfinal\\_4.pdf](https://yukon.ca/sites/yukon.ca/files/cs/2022-03-24_ml-floodmitigationoptionsfinal_4.pdf)
- van Drecht, L.H., Beranek, L.P., Colpron, M. and Wiest, A.C., 2022. Development of the Whitehorse trough as a strike-slip basin during Early to Middle Jurassic arc-continent collision in the Canadian Cordillera: Geosphere, vol. 18, no. 5, p. 1538– 1562. <https://doi.org/10.1130/GES02510.1>
- Varnes, D.J., 1978. Slope Movement Types and Processes. Special Report 176: Landslides: Analysis and Control. National Research Council, Transportation Research Board, Washington D.C., p. 11-33. <https://onlinepubs.trb.org/Onlinepubs/sr/sr176/176-002.pdf>

- Vreeken, W.J., 1981. Distribution and chronology of freshwater marls between Kingston and Belleville, Ontario. *Canadian Journal of Earth Sciences*, vol. 18, p. 1228-1239. <https://doi.org/10.1139/e81-114>
- Wheeler, J.O., 1961. Whitehorse Map-Area, Yukon Territory. Geological Survey of Canada, Memoir 312, 156 p.
- Wolfe, S., Bond, J. and Lamothe, M., 2011. Dune stabilization in central and southern Yukon in relation to early Holocene environmental change, northwestern North America. *Quaternary Science Reviews*, vol. 30, p. 324-334.
- Yarnell, J.M., Stanley, G. and Hart, C.J.R., 1999. New paleontological investigations of upper Triassic shallow-water reef carbonates (Lewes River Group) in the Whitehorse area, Yukon. In: Yukon Exploration and Geology 1998, C.F. Roots and D.S. Emond (eds.), Exploration and Geological Services Division, Yukon, Indian and Northern Affairs Canada, p. 179-184. [https://ygsftp.gov.yk.ca/publications/yeg/yeg98/yarnell\\_lewes\\_river.pdf](https://ygsftp.gov.yk.ca/publications/yeg/yeg98/yarnell_lewes_river.pdf)
- Yukon Geological Survey, 2020. Surficial geology dataset. Yukon Geological Survey, <https://data.geology.gov.yk.ca/Compilation/33> [accessed January 9, 2023].
- Yukon Geological Survey, 2022. Yukon Digital Bedrock Geology, [http://www.geology.gov.yk.ca/update\\_yukon\\_bedrock\\_geology\\_map.html](http://www.geology.gov.yk.ca/update_yukon_bedrock_geology_map.html) [accessed December 6, 2022].
- Yukon Water Resources Branch, 2022. Yukon Snow Survey Bulletin and Water Supply Forecast, May 1, 2022. Department of Environment, Government of Yukon. [https://yukon.ca/sites/yukon.ca/files/env/snow\\_bulletin\\_may\\_2022\\_en.pdf](https://yukon.ca/sites/yukon.ca/files/env/snow_bulletin_may_2022_en.pdf)

## **Appendix 1 – Map sheets**

The appendices are only available as digital files. They are included in a .zip file that accompanies this document, and are available from <https://data.geology.gov.yk.ca>.

### **1:15 000 scale surficial geology maps**

Sheet 1: Grizzly Valley area

Sheet 2: Shallow Bay area

Sheet 3: Ibex Valley area

Sheet 4: Takhini Hot Springs Road area

Sheet 5: City of Whitehorse (north)

Sheet 6: City of Whitehorse (central)

Sheet 7: Fish Lake

Sheet 8: City of Whitehorse (south)

Sheet 9: Goldenhorn area

Sheet 10: Army Beach, Marsh Lake area

### **1:25 000 scale aggregate potential map**

Sheet 11: Greater Whitehorse aggregate potential map

## Appendix 2 – Digital spatial data compilation

Accompanying zip file 'OF2023-1\_appendix2.zip' contains the following files:

- Geodatabase file 'OF2023\_1.gdb' contains four feature classes:
  - Surficial\_points (see Fig. 22 for feature types and symbology)
  - Surficial\_lines (see Fig. 23 for feature types and symbology)
  - Surficial\_polygons (see Fig. 24 for feature types and symbology)
  - Map\_extent
  
- ArcMap project file 'OF2023\_1.mxd' contains geodatabase layers above with standardized symbology.
  
- ArcMap layer files:
  - surficial\_points (all).lyr
  - surficial\_points water wells (overburden depth, m).lyr
  - surficial\_lines\_TYPE\_VALIDITY.lyr (geological boundaries only)
  - surficial\_lines\_TYPE\_SUBTYPE.lyr (other lines)
  - surficial\_polygons.lyr
  - surficial\_polygons\_aggregate\_potential.lyr
  - aggregate.lyr (group layer containing aggregate-related point, line, and polygon features)
  - landslides.lyr (group layer containing landslide-related point, line, and polygon features)
  - permafrost.lyr (group layer containing permafrost-related point, line, and polygon features)
  
- Symbology fonts:
  - gsc3.ttf
  - gsc4.ttf

Note that these custom fonts must be installed on your computer for standardized point symbology to display. To install the fonts, double click them in Windows Explorer/file manager and press 'install', or copy them into your system font folder (usually located at C:\Windows\Fonts).







**Yukon Geological Survey  
Energy, Mines and Resources  
Government of Yukon**

